Investigation of the Operation

of the

X-Ray/EPS Sensors on

GOES-4, -5, and -6,

Including a Comparison with NOAA8 Data

PANAMETRICS, INC.
221 Crescent Street
Waltham, Massachusetts 02254

Final Report

February 10, 1987

Prepared for

NOAA/ERL/SEL
325 Broadway
Boulder, Colorado 80303

Under Contract No. NA84RAC05108

TABLE OF CONTENTS

i

TABLE OF CONTENTS

LIST OF ILLUSTRATIONS (Cont'd)

LIST OF TABLES (Cont'd)

LIST OF TABLES

7. SOLAR X-RAY SENSOR (XRS) CHARACTERISTICS

The solar x-ray sensor (XRS) for GOES-4, -5, -6, -G, and -H is shown in the isometric view of Fig. 7.1. A functional block diagram of the XRS is shown in Fig. 7.2. The XRS measures solar x-rays in two bands of about 0.5-3 A° (A channel) and 1-8 A° (B channel). This is accomplished by use of a dual ion chamber as shown in the XRS telescope side view in Fig. 7.3 and the ion chamber properties listed in Table 7.1. The ion chamber response curves are shown in Fig. 7.4. The ion chamber theoretical responses have been verified by data given in Ref. 13, while the GOES-4, -5, and -6 ion chamber calibrations with Fe-55 sources (~ 2 A° x-rays) are given in Ref. 14, and the GOES-6 and -H ion chamber calibrations are given in Ref. 15.

The XRS data processing electronics are outlined in Fig. 7.5. The solar x-ray signal forms a current pulse as the XRS telescope view axis is swept past the sun once per spacecraft rotation (about 0.6 second). A spacecraft-provided on-sun pulse gates the demodulation electronics to allow measurement of the solar x-ray pulse. The wideband background output allows the solar x-ray pulse shape to be measured over many spacecraft rotations, and is used primarily as a diagnostic output. The narrowband background channel provides the average ion chamber current output. The GOES space environment can include large fluxes of high energy electrons (> 2 MeV) so the ion chambers are shielded by lead to reduce bremsstrahlung response, and by magnets in the aperture to reduce the direct electron response. The x-ray channel is largely immune from electron flux effects, but the background channels both show electron flux induced currents. The narrowband background channel can at times be dominated by electron flux produced currents. The GOES XRS units respond primarily to solar x-rays, but an intense, strongly spin-modulated electron flux can also affect the x-ray flux output. The latter is generally rare, and has the larger effect on the A channel.

The XRS telemetry output voltages are converted to fluxes and currents through constants given in a Calibration Report provided with each XRS unit. These constants are generally given for +25°C, -10°C, and +30°C. The x-ray flux covers a wide dynamic range, 10^{-9} to 10^{-4} W/m^2 for channel A and 10^{-8} to 10^{-3} W/m^2 for channel B, so the x-ray telemetry output is one analog voltage (V_x) and two range bits. The range bits cover four gain levels for V_x (range bits 0 to 3) with adjacent range sensitivity changing by approximately a factor of 10. The x-ray flux for a telemetry voltage V_x in range R (0 to 3) is given by

$$J_x(W/m^2) = (V_x - C_x(T))/(S_x(T) K) \qquad (7.1)$$

where T is the XRS telescope temperature. The temperature corrected calibration constants are given by

and

$$C_x(T) = C_x + DC_x (25-T)/35 \qquad (7.2)$$

$$S_x(T) = S_x + DS_x (25-T)/35 \qquad (7.3)$$

73

Solar X-Ray
Sensor Electronics

S/C Connector (not
shown) protrudes
through bottom of unit

Solar X-Ray
Sensor Telescope

Magnet Yoke

Magnet

Positioner
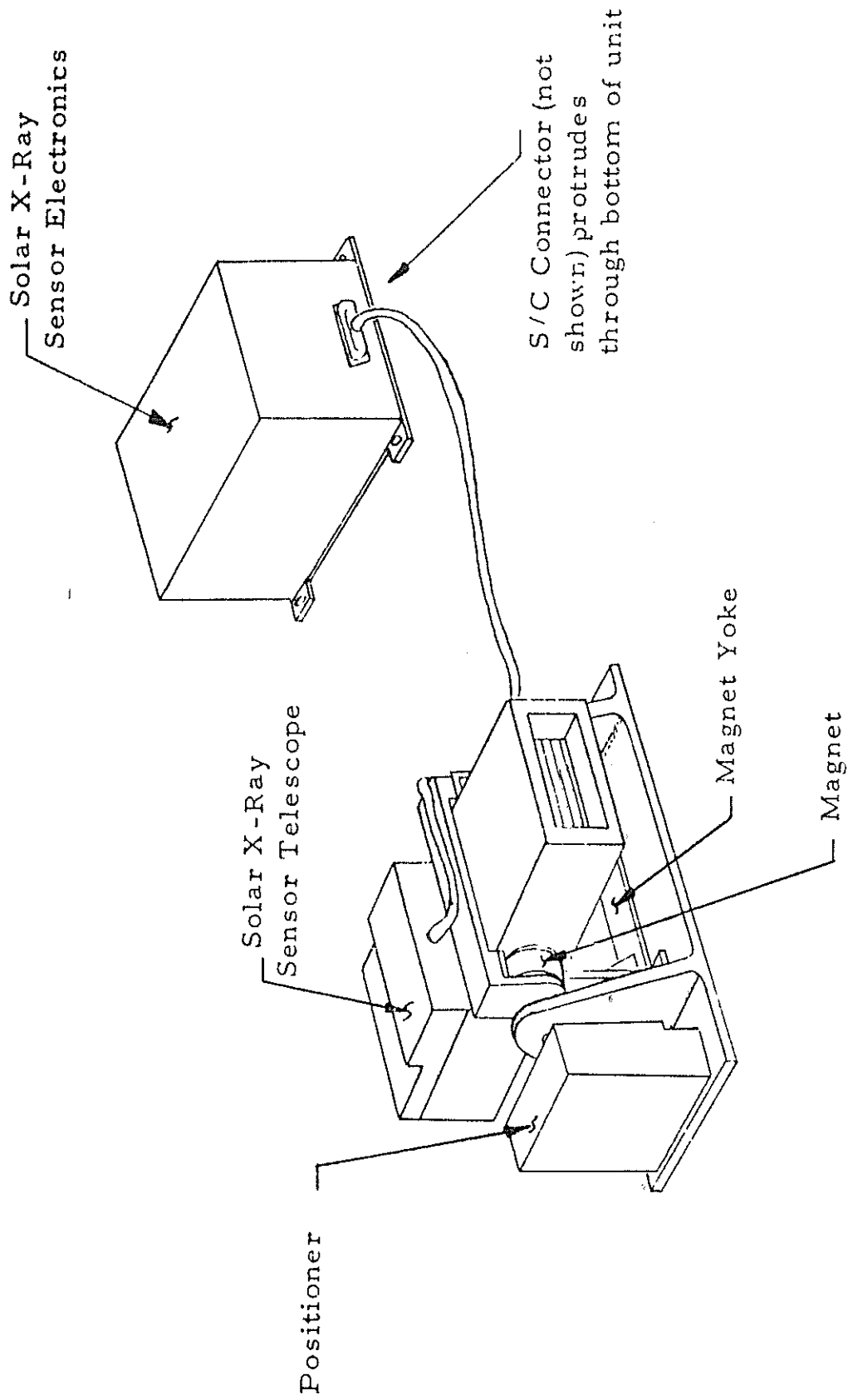
Figure 7.1.   Solar X-Ray Sensor Subsystem.

SOLAR X-RAY SENSOR

TELESCOPE

COLLIMATOR | ION CHAMBERS | PICOAMPERE PREAMPLIFIERS

DPU ELECTRONICS

DATA PROCESSOR

CALIBRATION

AUTORANGING LOGIC

TIMING LOGIC

REGULATED POWER SUPPLY

SOLAR X-RAYS

X-RAY SENSOR CALIBRATION ON
X-RAY SENSOR CALIBRATION OFF

X-RAY SENSOR OFF
X-RAY SENSOR ON

2048 SPIN PULSES

ON-SUN PULSE

POWER

X-RAY SENSOR TEMPERATURE
X-RAY SHORT SUN
X-RAY SHORT BACKGROUND (WB)
X-RAY LONG SUN
X-RAY LONG BACKGROUND (WB)
X-RAY SHORT BACKGROUND (NB)
X-RAY LONG BACKGROUND (NB)
X-RAY ELECTRONICS TEMPERATURE
X-RAY SHORT SCALE (MSB)
X-RAY SHORT SCALE (LSB)
X-RAY LONG SCALE (MSB)
X-RAY LONG SCALE (LSB)
X-RAY REFERENCE VOLTAGE
X-RAY CALIBRATION/DATA

Figure 7.2. XRS Functional Block Diagram.

75
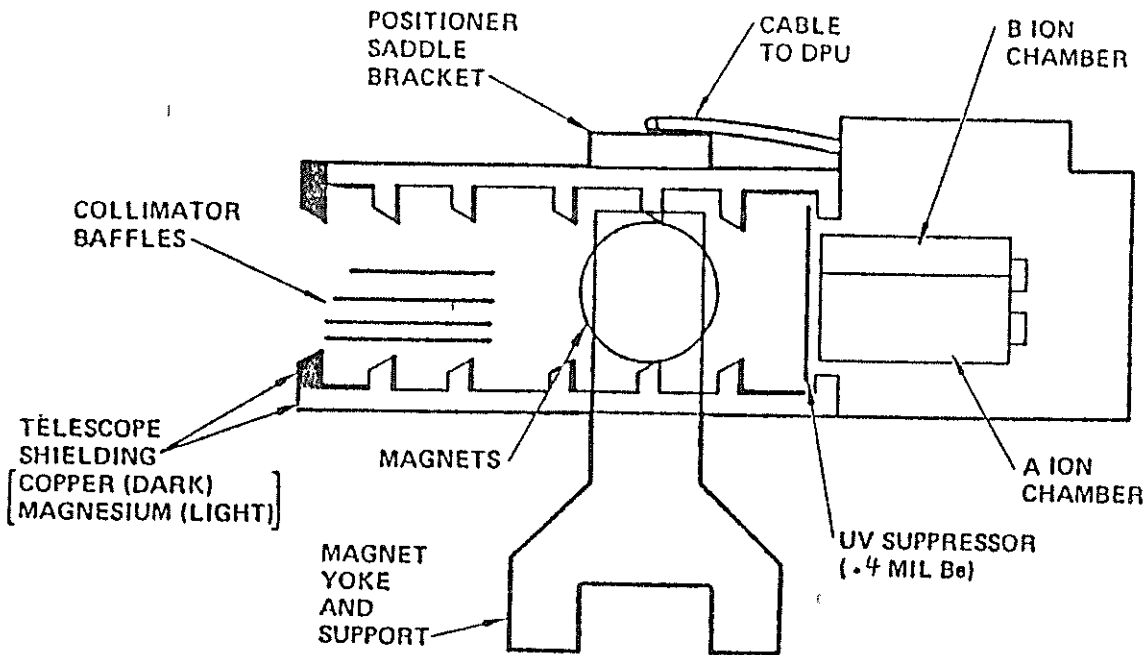
Figure 7.3. X-Ray Sensor Telescope Side View.

Table 7.1

Ion Chamber Properties

Characteristic	Chamber A Value	Chamber B Value
Nominal x-ray range ($\overset{\circ}{A}$)	0.5 - 3	1 - 8
Window thickness - Be (mils) (nominal)	20	2
Gas fill (Component/%)	Xe/99.6, He/0.3	Ar/99.6, He/0.4
Fill pressure (mm Hg at 25°C)	180	800
Window width, w (in/cm)	0.75/1.91	0.25/0.64
Window area, a(cm^2)	5.80	1.90
Chamber depth (cm)	3.99	3.99
Effective gas density for x-ray absorption (mg/cm^3 (type))	1.255 (Xe)	1.712 (Ar)
Total gas thickness, t_g (mg/cm^2)	5.051 (Xe)	6.831 (Ar)
1/e depth for Fe-55 x-rays, 1/(cm)	1.17	2.21
Energy to produce an electron-ion pair, W(eV/pair)	22.0 (Xe)	26.2 (Ar)
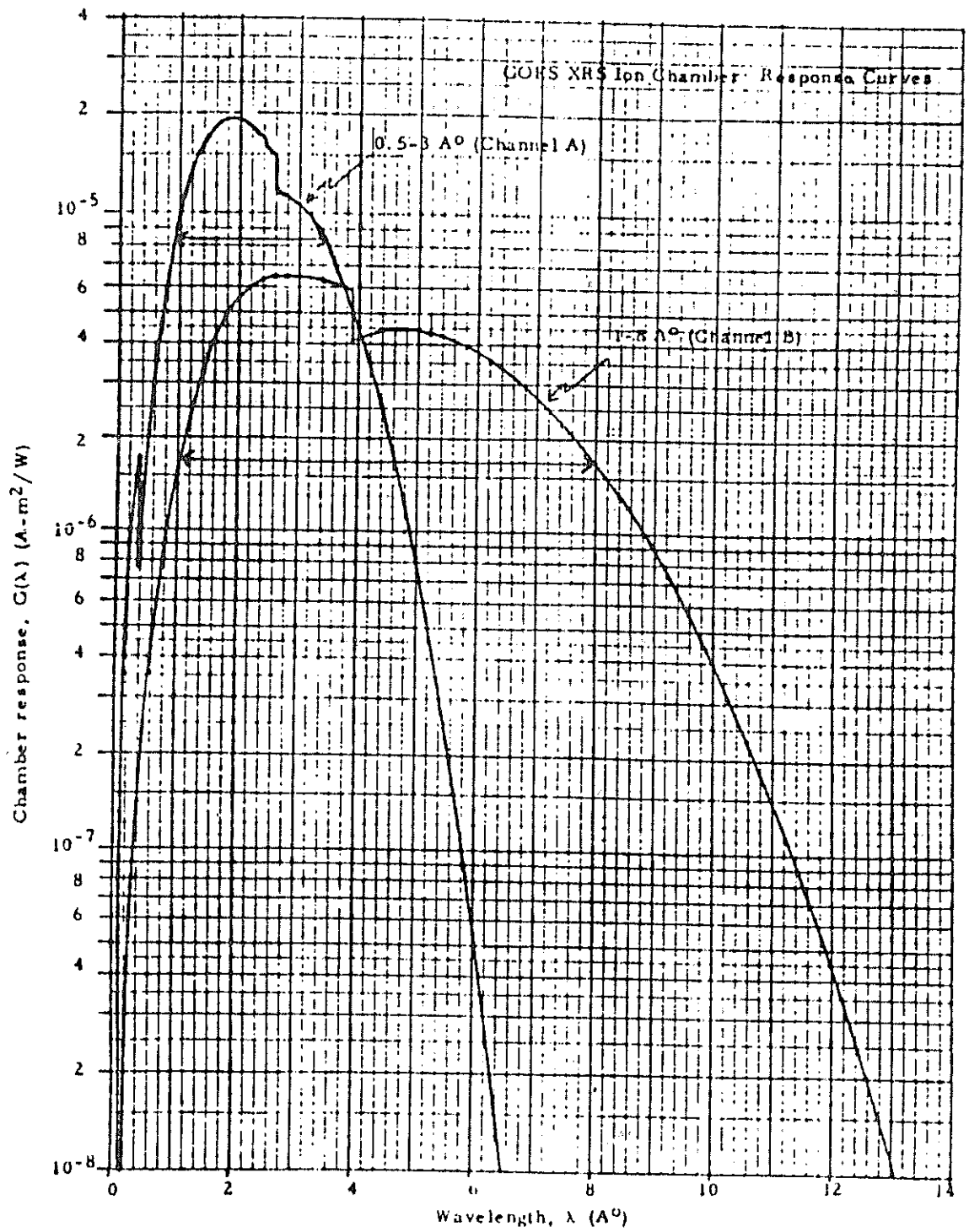
Figure 7.4. Ion Chamber Response Curves for X-Rays.
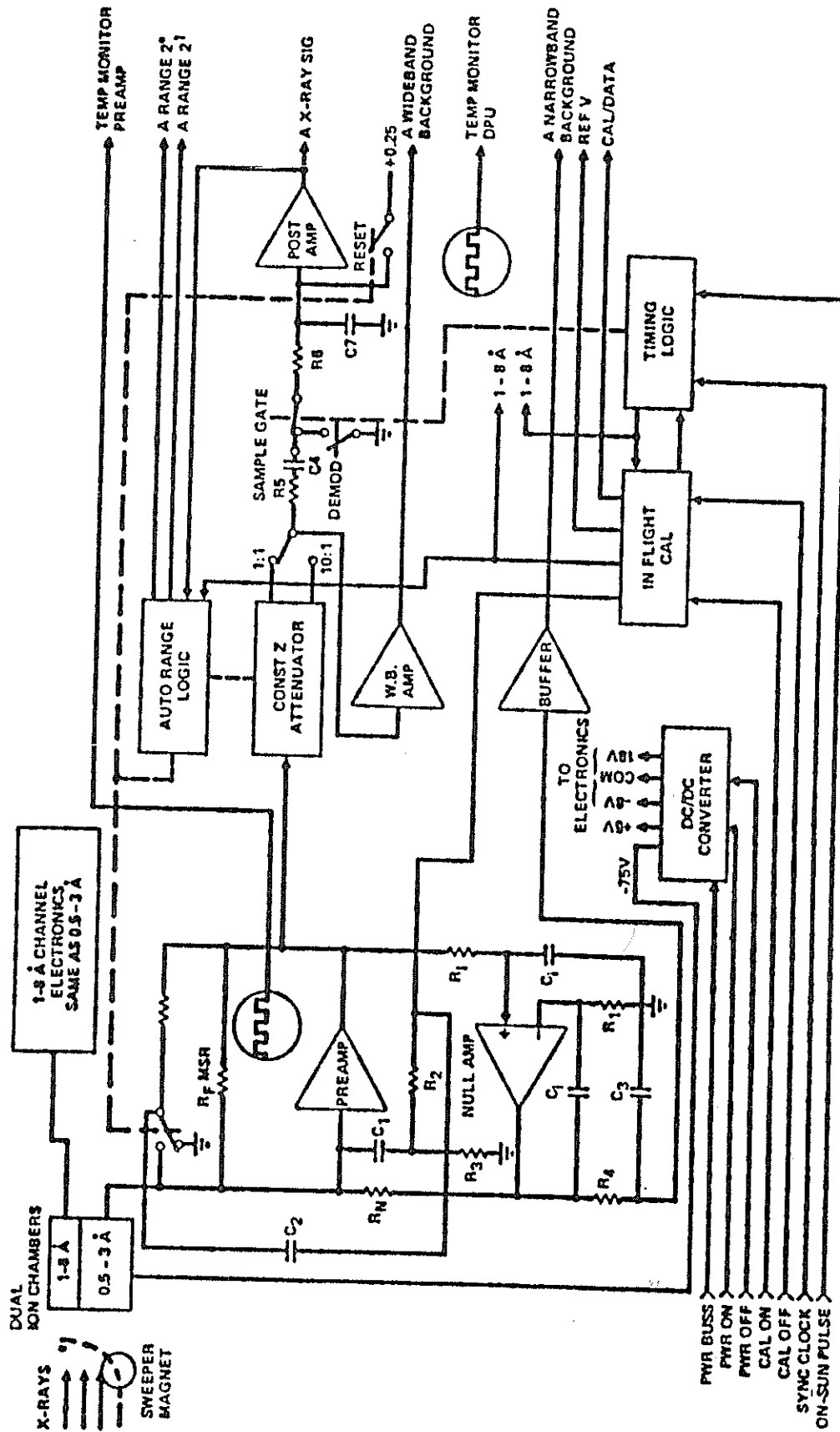
Figure 7.5. Block Diagram of Data Processing Electronics.

78

where C_x and S_x are the 25°C values. The x-ray channel calibration constants are given in Table 7.2 for GOES-4, -5, -6, and -H (the -G unit was destroyed in the May 1986 launch vehicle failure). For most operations it is sufficiently accurate to use only the 25°C values in (7.1). The DC_x and DS_x values in Table 7.2 are based on the -10°C and +25°C Calibration Report data (-20°C data for GOES-4).

The narrowband background current is given by

$$I_B(A) = (V_B - C_B(T))/S_B(T) \qquad (7.4)$$

where V_B is the telemetry voltage and the temperature corrected calibration constants are

$$C_B(T) = C_B + DC_B(25-T)/35 \qquad (7.5)$$

and

$$S_B(T) = S_B + DS_B(25-T)/35 \qquad (7.6)$$

The values for C_B, DC_B, S_B, and DS_B for GOES-4, -5, -6 and -H are given in Table 7.3. The wideband background telemetry voltage gives the preamplifier output voltage from

$$V_{PA} = (V_W - C_W)/G_W \qquad (7.7)$$

The preamplifier voltage is generally used to check the solar x-ray pulse waveform and the spin-modulated electron background current, so it is not directly calibrated in ion chamber current. This could be done by comparing the peak V_{PA} with the ion chamber current calculated from the V_x x-ray output. Note, however, that V_{PA} is an AC signal with the DC background subtracted.

The narrowband background current I_B is about 1/10 the x-ray flux current since the solar x-ray pulse is about 1/10 of a rotation width (36° FWHM; 10% duty cycle). Electron flux produced currents will raise I_B above the solar x-ray current level. This effect is discussed more fully in Section 10.

The XRS has a temperature monitor in the DPU and in the telescope, with linear fit coefficients being given in Table 7.4. These fits are based on the -10°C to +25°C data in the XRS unit Calibration Reports. As stated in Table 7.4, the fits are accurate to ± 1°C over the range -10°C to +25°C. For more accuracy outside this range the actual Calibration Report data should be used. Since most of the XRS signal temperature variations arise from the preamplifier and other electronics in the telescope, the telescope temperature should be used when the XRS data are corrected for temperature. For most normal data analysis the 25°C values of the calibration constants can be used. Only at -10°C do the values change by 5 to 10% (maximum). In-orbit operation shows that the XRS eclipse minimum temperatures are about 0°C.

Table 7.2

XRS Calibration Constants for X-Ray Channels

Chan/ Range	Mult.*	GOES-4		GOES-5		GOES-6		GOES-7	
		S_x	DS_x	S_x	DS_x	S_x	DS_x	S_x	DS_x
A/R0	10^{12}	1.78	+0.10	1.85	+0.09	2.05	+0.14	1.90	+0.20
/R1	10^{11}	1.68	+0.12	1.76	+0.12	2.02	+0.15	1.85	+0.13
/R2	10^{10}	2.44	+0.11	2.30	+0.08	2.35	+0.07	2.50	+0.06
/R3	10^9	2.26	+0.08	2.13	+0.07	2.15	+0.06	2.28	+0.03
B/R0	10^{11}	5.85	+0.35	6.02	+0.33	6.06	+0.38	6.90	+0.49
/R1	10^{10}	5.47	+0.36	5.67	+0.41	5.71	+0.47	6.59	+0.20
/R2	10^9	7.60	+0.23	7.98	+0.21	8.06	+0.23	9.49	+0.52
/R3	10^8	7.00	+0.20	7.34	+0.18	7.35	+0.21	8.82	+0.20
A/K**	10^{-5}	1.73		1.74		1.74		1.68	
B/K**	10^{-6}	4.56		4.84		4.43		4.48	
A/C_x†	1	0.499	+0.009	0.498	+0.013	0.507	+0.010	0.510	+0.012
B/C_x	1	0.499	+0.012	0.497	+0.011	0.502	+0.016	0.519	+0.003

---

*Multiplier for all S_x and DS_x values.

**K Calibration constant values for each XRS unit
  (no temperature variation).

†C_x and DC_x values for each XRS unit.

Table 7.3

XRS Calibration Constants for Background Channels

Spacecraft/Channel	Wideband		Narrowband			
	G_W	C_W	S_B*	DS_B*	C_B	DC_B
GOES-4/A	10.23	2.34	3.23	+0.18	0.991	+0.002
/B	10.30	2.36	0.912	+0.054	0.997	-0.002
GOES-5/A	10.30	2.32	3.26	+0.17	0.986	-0.001
/B	10.20	2.33	0.893	+0.054	0.998	+0.002
GOES-6/A	10.29	2.35	3.35	+0.11	0.998	0.000
/B	10.26	2.34	0.917	+0.062	0.995	+0.001
GOES-H/A	10.3	2.35	3.30	+0.20	0.986	0.000
/B	10.3	2.35	0.898	+0.057	0.988	0.000

*Multiply S_B and DS_B by 10^{11}.

Table 7.4

XRS Temperature Monitor Linear Fit Coefficients

Spacecraft	DPU		Telescope	
	m	b	m	b
GOES-4	58.59	-111.8	62.37	-112.7
GOES-5	61.44	-107.1	63.37	-119.5
GOES-6	60.22	-114.6	59.10	-110.8
GOES-H	58.80	-112.2	64.25	-111.7

Note: Temperature = m x (Telemetry volts) + b = degrees C.

Fit is to +1°C over -10°C to +25°C.

81

The in-orbit operation of the XRS units on GOES-4, -5, and -6 is discussed in the following Sections. The in-flight calibration cycle data are discussed in Section 8, while the x-ray data are discussed in Section 9. The response of the XRS to the ambient electron flux is discussed in Section 10, and recommendations on in-orbit operations are given in Section 11.

8. IN-FLIGHT CALIBRATION CYCLE OF THE XRS

8.1 Description of the IFC Cycle

The in-flight calibration (IFC) cycle checks the gain and zero level of each of the four ranges in both x-ray channels. During the IFC the x-ray pulse timing is shifted by 180° to reduce interference from solar x-rays. The IFC checks all of the XRS electronics for proper operation. The IFC is initiated by ground command and terminated by ground command. A full cycle requires a minimum of 8 level steps taking about 5 minutes. The 8 IFC step cycle as shown in Table 8.1, which also lists the calibration constants for GOES-4, -5, -6 and -H. The 8 IFC steps repeat until the IFC off command is sent.

The IFC calibration constants in Table 8.1 are obtained from the thermal vacuum test data, which are included with the Calibration Report for each XRS unit. The V_{xc} values are for 25°C, while the DV_{xc} values are obtained from the 25°C and -10°C (-20°C for GOES-4) data. The V_{xc} (7) values are calculated as shown at the bottom of Table 8.1. In-orbit XRS temperatures vary from 10°C to 25°C, with eclipse minimums near 0°C, so the 25°C values V_{xc} should normally be sufficiently accurate. The maximum change in the high level values is about +7% at -10°C.

8.2 Use of Data from In-Orbit IFC Cycles

The in-orbit IFC data give a set of 8 measurement points for each x-ray channel. The simplest check is to compare the in-orbit values with the 25°C baseline values of Table 8.1 and monitor for < 5% change in all points. A better method is to measure the gain change for each range, and the zero level shift. From Table 8.1 it can be seen that the "lo" IFC step in all four ranges is nearly identical, both at 25°C and in temperature variation. The "lo" values are the output for a zero input current (neglecting any solar x-ray pulse tail effects) and are derived from the output offset voltage circuit, which is the same circuit for all ranges. Thus the four "lo" values should be identical, and can be averaged to provide a measurement of the offset voltage $C_x(T)$ in Eq. (7.1).

The "hi" values are measures of the range/channel gain, and are best compared by

$$R_g \quad (\text{"hi"}-\text{"lo"})/(\text{"hi"}-\text{"lo"})_{base} \qquad (8.1)$$

Table 8.1

IFC Calibration Constants for GOES-4, 5, 6, and H

Step	Range/Level	GOES-4 $\underline{V}_{xc}$	$\underline{DV}_{xc}$	GOES-5 $\underline{V}_{xc}$	$\underline{DV}_{xc}$	GOES-6 $\underline{V}_{xc}$	$\underline{DV}_{xc}$	GOES-H $\underline{V}_{xc}$	$\underline{DV}_{xc}$
Channel A									
1	R3/hi	3.220	0.077	3.128	0.090	2.949	0.091	2.920	0.078
2	R3/lo	0.497	0.012	0.498	0.012	0.506	0.011	0.521	0.000
3	R2/hi	3.040	0.077	2.949	0.088	2.776	0.087	2.902	0.094
4	R2/lo	0.496	0.013	0.497	0.013	0.506	0.011	0.518	0.005
5	R0/hi	2.330	0.140	2.702	0.162	2.755	0.169	2.665	0.187
6	R1/hi	2.532	0.159	2.897	0.175	2.978	0.189	2.740	0.165
7	R1/lo	0.495	0.012	0.497	0.013	0.507	0.009	0.520	−0.001
8	R0/lo	0.494	0.012	0.498	0.013	0.505	0.010	0.510	0.013
Channel B									
1	R3/hi	3.653	0.112	3.555	0.093	3.334	0.101	3.656	0.060
2	R3/lo	0.497	0.014	0.496	0.012	0.502	0.016	0.522	0.000
3	R2/hi	3.432	0.110	3.336	0.089	3.134	0.096	3.599	0.105
4	R2/lo	0.496	0.014	0.496	0.012	0.502	0.016	0.523	0.001
5	R0/hi	2.703	0.169	2.700	0.160	2.495	0.160	2.842	0.099
6	R1/hi	2.882	0.193	2.902	0.167	2.678	0.181	2.869	0.064
7	R1/lo	0.498	0.012	0.496	0.012	0.502	0.015	0.522	0.000
8	R0/lo	0.492	0.018	0.496	0.013	0.501	0.014	0.521	0.002

Note: V_{xc} is the value at 25°C, and $V_{xc}(T) = V_{xc} + DV_{xc}(25-T)/35$.

where ("hi"-"lo")$_{base}$ can be either the 25°C values or the
temperature corrected values using the XRS sensor (telescope)
temperature, both obtained from Table 8.1. The R_g values from
(8.1) have solar x-ray pulse tail and modulated electron background
effects cancelled to first order, and so give a more reliable gain
measure than the "hi" value alone.

The "lo" values are generally affected by solar x-ray fluxes
and electron background, especially in the lowest range R0. The
solar x-ray pulse is generally shaped so that the IFC tail is
less than 10% of the x-ray peak. The "lo" offset voltage is near
0.5 V, so ± 5% stability is ± 0.025 V, which corresponds to a
0.25 V x-ray signal (0.75 V including the offset). Thus the "lo"
IFC value is not a valid test if the on-sun x-ray signal is >
0.75 V in that range or > 3 V in the next lower range (there is
about a factor of 10 gain change between adjacent ranges). The
"lo" IFC values should be averaged only over the valid ranges.

Large solar x-ray fluxes (R3 or R2) can invalidate most of
the IFC data. The R0 value of R_g (8.1) may well be invalid
because the "hi" value saturates at 5.11 V on the telemetry
readout. The IFC data should only be used routinely if the solar
x-ray flux is in R1 or R0, preferably in R0.

*

The electron background can also affect the IFC if a strong
spin-modulation is present. This will generally affect the low
ranges (R0 and possibly R1), and should not be a common accurate-   *occurance,*
ness. Large electron fluxes (large EPS E1 counts) will also
increase the statistical variations of the "lo" values in R0 for
the A channel and perhaps the B channel, thus making it difficult
to obtain an accurate measurement. The effects of electron
background are described in more detail in Sections 8.1 and 10.
The following Section 8.3 also presents the long term in-orbit
IFC stability data for the GOES-4, 5 and 6 XRS units.

8.3   Long Term IFC Data for GOES-4, -5, and -6

The GOES-4, -5 and -6 spacecraft were launched in September
1980, May 1981, and May 1983, as shown in Table 3.8. The XRS
turn-on was about the same as the EPS turn-on. The GOES-4
spacecraft was used minimally after the GOES-6 launch since the
GOES-4 VAS failed in November 1982, and the XRS was off for a
number of years. In June 1986 the GOES-4 XRS was turned on for
about 2 weeks and some IFC data obtained after almost six (6)
years in orbit.

The GOES-4 IFC data for 14 September 1981 and 21 June 1986
are given in Table 8.2. The gain (R_g from Eq. (8.1)) and "lo"
values are both compared with the 25°C base values in Table 8.1.
The 1981 IFC data show some solar x-ray pulse effects on the "lo"
values in R0 (A and B channels) and R1 (B channel). Note that
the 1-4% "lo" values have 0.005 to 0.022 V shifts on telemetry,
which has 1 bit for 0.010 V resolution. The A/B "lo" values show
an average shift of -0.006 V/-0.007 V for 1981 and -0.016 V/
-0.018 V for 1986.

84

Table 8.2

GOES-4 In-Orbit IFC Data

Channel /Range	14 Sept. 1981/1940 UT			21 June 1986/1705 UT		
	R_g (8.1)	1o/base	1o-base	R_g (8.1)	1o/base	1o-base
A/R3	1.003	0.986	−0.007	1.006	0.966	−0.017
A/R2	1.002	0.988	−0.006	1.002	0.968	−0.016
A/R1	1.026	0.990	−0.005	1.009	0.966	−0.017
A/R0	1.026	(1.079)	(+0.039)	1.014	0.974	−0.013
A x-ray (V(R))	1.090 (R0)			0.49 (R0)		
B/R3	1.011	0.986	−0.007	1.007	0.970	−0.015
B/R2	1.008	0.988	−0.006	1.004	0.968	−0.016
B/R1	1.032	(1.044)	(+0.022)	1.013	0.964	−0.018
B/R0	1.022	(1.728)	(+0.358)	1.000	0.955	−0.022
B x-ray (V(R))	0.990 (R1)			0.49 (R0)		
Approx. tel. temp.	19°C			15°C		
E1 (cnts/readout)	47			6.3		

Note: (1o/base) and (1o-base) numbers in parentheses are contami-
nated by the solar x-ray pulse tail.

The gain values in Table 8.2 show that R3/R2 and R1/R0 are nearly the same, as is expected since most of the gain change comes from the high resistance (about 10^{12} ohms) feedback resistors in the XRS preamplifiers. The preamplifier gains are the same for the R3/R2 and the R1/R0 range pairs. The higher gain ranges (R1/R0) for both the A and B channels show about a 2 1/2% increase in 1981, and a 1% increase in 1986. These variations are close to that expected for the temperature differences between the in-orbit data and the 25°C TV data in Table 8.1. The lower gain ranges (R3/R2) show shifts of 1% or less and are stable to < 1% over a nearly 6 year period.

GOES-5 XRS IFC data for 3 October 1986 are shown in Table 8.3, and illustrate the magnitude of temperature effects. These data are for the post-eclipse minimum temperature of 6.6°C. The data are compared with both the +25°C TV base and the +6.5°C base (+25°C and -10°C TV average). The temperature adjusted base is clearly needed if < 1% accuracy is required, since the R3/R2 gain shift is about 1.5% and the R1/R0 gain shift is about 3.5%. If IFC data are to be used to correct the in-orbit gains, then it is best to use the temperature corrected base. Normal IFC data are usually taken near 1800 UT when the XRS is near 10 to 25°C, depending on the season, so the non-temperature-corrected IFC data will generally give at least 2% accuracy when compared with the +25°C TV base.

The temperature-corrected IFC data should be used only if the XRS x-ray fluxes are also temperature corrected, since the magnitude of the variations are comparable. This would require using (7.2) and (7.3) in (7.1) to calculate the flux, with an additional gain adjustment factor for (7.3) given by (8.1) as

$$S_x(T)_{corr} = S_x(T) \; R_g(range) \qquad\qquad (8.2)$$

where R_g (range) is for the R3/R2 or R1/R0 range pairs, and with an offset voltage correction of

$$C_x(T)_{corr} - C_x(T) + DLB \qquad\qquad (8.3)$$

where DLB is the average of the (1o-base) values, corrected for temperature, as listed in Table 8.2 for GOES-4. The use of these corrections is discussed in Section 11. For most operations the use of 25°C TV calibration constants with no temperature or IFC shift corrections should be sufficiently accurate, since the total corrections should be < 5%, and usually < 3%.

The GOES-5 in-orbit IFC gain history is shown in Table 8.4. The listed temperatures are mostly estimates based on the observed annual variations of the XRS telescope (sensor) temperature for 1981-82, except for the October 1986 data which are actual measured sensor temperatures during the IFC. The 3 October 1986 data were shown in Table 8.3 to illustrate temperature variations. The (R3/R2) range pair gain is seen to be stable to better than

Table 8.3

GOES-5 In-Orbit IFC Data Showing Temperature Effects

3 October 1986/0555 UT - Post eclipse minimum temp.

Channel/Range	base = 25°C TV		base = +6.5°C	
	R_g (8.1)	1o/base	R_g (8.1)	1o/base
A/R3	1.015	0.984	1.000	0.972
A/R2	1.011	0.986	0.996	0.972
A/R1	1.010	0.986	0.977	0.972
A/R0	1.014	(1.034)	0.981	(1.020)
A x-ray (V(R))	0.480 (R0)			
B/R3	1.010	0.988	0.996	0.976
B/R2	1.008	0.988	0.994	0.976
B/R1	1.014	0.988	0.983	0.976
B/R0	1.009	0.988	0.976	0.974
B x-ray (V(R))	0.536 (R0)			
Meas. tel. temp.	+6.6°C			
E1 (cnts/readout)	73.7			

Table 8.4

GOES-5 In-Orbit IFC Gain History

R_g (8.1) gain values relative to 25°C TV base. and average values for (R3/R2) and (R1/R0) gain pairs

Channel /Range	4JUN81 1730UT	5JUN81 1500UT	5SEP81 1740UT	16OCT82 1810 UT	20AUG85 1820 UT	8OCT85 1810UT	10JUN86 1810 UT	17JUN86 1810 UT	2OCT86 0610UT	3OCT86 0555UT
A/R3	1.007	1.015	1.011	1.006	1.007	1.004	1.010	1.010	1.015	1.015
A/R2	1.007	1.011	1.011	1.005	1.006	1.003	1.006	1.005	1.011	1.011
A/R1	0.987	0.994	1.011	0.995	0.990	0.985	0.992	0.993	1.010	1.010
A/R0	0.978	0.990	1.007	0.990	1.018	0.988	0.990	1.004	1.021	1.014
A/(R3/R2)	1.007	1.013	1.001	1.006	1.007	1.004	1.008	1.008	1.013	1.013
A/(R1/R0)	0.983	0.992	1.009	0.993	1.004	0.987	0.991	0.999	1.016	1.012
B/R3	1.006	1.010	1.008	1.004	1.004	1.000	1.004	1.005	1.010	1.010
B/R2	1.005	1.007	1.007	1.001	1.001	0.996	1.004	1.004	1.007	1.008
B/R1	0.951	0.955	1.015	1.000	0.997	0.989	1.000	1.002	1.014	1.014
B/R0	0.931	0.938	1.018	0.998	0.997	0.990	1.004	0.999	1.010	1.009
B/(R3/R2)	1.006	1.009	1.008	1.003	1.003	0.998	1.004	1.005	1.009	1.009
B/(R1/R0)	0.941	0.947	1.017	0.999	0.997	0.990	1.002	1.001	1.012	1.012
Approx. temp	(10°C)	(10°C)	(17°C)	(17°C)	(17°)	(17°)	(10°C)	(10°C)	6.6°C	6.6°C

1% of the +25°C TV base, for both channels A and B. The (R1/R0) range pair gain for channel A is stable to ± 1.5% over the 5.3 years, but may be 2% below the pre-launch TV data as shown in Table 8.3. The channel B (R1/R0) gain shows an initial 5-6% decrease which is recovered within 3 months, and thereafter is stable to ± 1.5%. The Table 8.3 temperature corrected data show that the B(R1/R0) gain may be 2% below the pre-launch TV data. The initial decrease and recovery of the B(R1/R0) gain may be from moisture or some other contamination of the high megohm preamp feed-back resistor, which slowly evaporated to recover nearly the pre-launch value.

The IFC offset history for GOES-5 is shown in Table 8.5. The 1o/base values in parenthesis have either a solar x-ray pulse or modulated electron background effect and are not included in the listed average or the (1o-base) average. The A and B channels both show stable offsets which are about 0.010 V below the 25°C TV base value. The temperature corrected offsets for 3 October 1986 (also shown in Table 8.3) show that temperature is not a large factor in the measured offsets. The offset shift of about -0.010 V is only 1 LSB in the 9 bit telemetry word for the x-ray signal voltage. The offset shift of about 2% is thus near the resolution of the telemetry data, and is 2% only because the offset voltage is 0.5 V. In practice, the offset shift corresponds to 2% of the x-ray flux at the low trip point in R3, R2 and R1, and becomes less as the x-ray signal voltage increases. For normal operation using the 25°C calibration constants, the offset shift can be neglected.

The GOES-6 IFC gain history is shown in Table 8.6, which has the same format as Table 8.4. The (R3/R2) gains are stable to < 1% over 3.3 years, and the temperature corrected data for 3 October 1986 show less than 0.5% shift from the pre-launch TV calibrations. The (R1/R0) gains for channel B are also stable to < 1%, with < 0.5% shift for 3 October 1986, but may have had an initial 3% change (this could possibly be a temperature effect). The channel A (R1/R0) gain is about 3% low after 3.3 years, but has been stable to 1% except for a possible initial 3% shift (may be a temperature effect). The (R1/R0) initial gain shifts are likely to be initial outgassing and contamination removal effects, as observed for the GOES-5 XRS.

The GOES-6 IFC offset history is shown in Table 8.7, with the last entry set being the temperature corrected offsets for 3 October 1986. The offsets appear to be stable at about 0.010 V below the TV base values, about 1 LSB in the telemetry word. The GOES-5 and GOES-6 XRS units show about the same in-orbit stability characteristics. For routine operation, the +25°C TV calibration constants should provide x-ray fluxes which differ by no more than ± 3% from the temperature corrected fluxes.

Table 8.5

GOES-5 In-Orbit IFC Offset History

1o/base for 25°C TV base; average; 1o-base in volts (V)

Channel /Range	4JUN81 1730UT	5JUN81 1500UT	5SEP81 1740UT	16OCT82 1810 UT	20AUG85 1820 UT	8OCT85 1810UT	10JUN86 1810 UT	17JUN86 1810 UT	2OCT86 0610UT	3OCT86 0555UT	3OCT86 (to+6.5°C 0555UT base)
A/R3	0.987	0.967	0.984	0.974	0.972	0.964	0.972	0.972	0.984	0.984	0.972
A/R2	0.986	0.966	0.986	0.976	0.972	0.966	0.978	0.982	0.986	0.986	0.972
A/R1	0.986	0.982	(1.012)	0.972	0.986	0.984	0.986	0.986	0.986	0.986	0.972
A/R0	(1.010)	(1.004)	(1.211)	0.984	0.984	(1.014)	(1.044)	0.974	1.000	(1.034)	(1.020)
$\bar{A}$(average)(#)	0.986(3)	0.972(3)	0.985(2)	0.977(4)	0.979(4)	0.971(3)	0.979(4)	0.979(4)	0.989(4)	0.985(3)	0.972(3)
$\bar{A}$(1o-base)(V)	-0.007	-0.014	-0.008	-0.012	-0.011	-0.015	-0.011	-0.011	-0.006	-0.008	-0.014
B/R3	0.986	0.971	0.982	0.968	0.968	0.966	0.968	0.968	0.988	0.988	0.976
B/R2	0.968	0.968	0.988	0.974	0.968	0.971	0.968	0.968	0.988	0.988	0.976
B/R1	0.974	(0.994)	(1.250)	0.998	0.968	0.968	0.974	0.968	0.988	0.988	0.976
B/R0	0.994	(1.159)	(3.688)	(1.230)	(1.004)	0.984	0.988	0.994	0.994	0.988	0.974
$\bar{B}$(average)	0.981(4)	0.970(2)	0.985(2)	0.980(3)	0.968(3)	0.972(4)	0.975(4)	0.975(4)	0.990(4)	0.988(4)	0.976(4)
$\bar{B}$(1o-base)(V)	-0.010	-0.015	-0.007	-0.010	-0.016	-0.014	-0.013	-0.013	-0.005	-0.006	-0.012

Table 8.6

GOES-6 In-Orbit IFC Gain History

R_g (8.1) gain values relative to 25°C TV base, and average values for (R3/R2) and (R1/R0) gain pairs

Channel /Range	18MAY83 2145 UT	19AUG85 1840 UT	9JUN86 1840UT	29SEP86 1840 UT	2OCT86 0740UT	3OCT86 0735UT	3OCT86(to6.5°C 0735 UT base)
A/R3	1.015	1.009	1.010	1.007	1.015	1.015	0.999
A/R2	1.014	1.007	1.009	1.004	1.013	1.012	0.996
A/R1	1.018	0.988	0.993	0.986	1.005	1.004	0.968
A/R0	1.037	0.985	0.989	0.978	0.999	1.001	0.967
A/(R3/R2)	1.015	1.008	1.010	1.006	1.014	1.014	0.998
A/(R1/R0)	1.028	0.987	0.991	0.982	1.002	1.003	0.968
B/R3	1.013	1.009	1.010	1.006	1.013	1.013	0.999
B/R2	1.014	1.007	1.008	1.003	1.014	1.011	0.996
B/R1	1.029	1.015	1.019	1.009	1.031	1.029	0.992
B/R0	1.036	1.009	1.014	1.002	1.028	1.029	0.993
B/(R3/R2)	1.014	1.008	1.009	1.005	1.014	1.012	0.998
B/(R1/R0)	1.033	1.012	1.017	1.006	1.030	1.029	0.993
Approx.temp.	(15°C)	(17°C)	(10°C)	16.8°C	5.6°C	6.2°C	6.2°C

Table 8.7

GOES-6 In-Orbit IFC Offset History

Channel /Range	1o/base for 25°C TV base; average; 1o-base in volts (V)						
	18MAY83 2145 UT	19AUG85 1840 UT	9JUN86 1840UT	29SEP86 1840 UT	2OCT86 0740UT	3OCT86 0735UT	3OCT86(to6.5°C 0735 UT base)
A/R3	0.988	0.978	0.980	0.968	0.988	0.988	0.977
A/R2	0.988	0.974	0.972	0.968	0.988	0.988	0.977
A/R1	0.994	0.969	0.974	(0.941)	0.986	0.986	0.977
A/R0	(0.937)	0.980	0.950	(0.733)	0.986	0.976	0.965
(average)(#)	0.990(3)	0.975(4)	0.969(4)	0.968(2)	0.987(4)	0.985(4)	0.974(4)
(1o-base)(V)	−0.006	−0.012	−0.015	−0.016	−0.006	−0.008	−0.014
B/R3	0.996	0.979	0.976	0.980	0.996	0.996	0.980
B/R2	0.996	0.976	0.976	0.976	0.996	0.996	0.980
B/R1	(1.041)	0.979	0.980	0.970	0.996	0.996	0.980
B/R0	(1.387)	0.978	0.982	(0.918)	0.984	0.994	0.978
(average)(#)	0.996(2)	0.978(4)	0.979(4)	0.975(3)	0.993(4)	0.996(4)	0.980(4)
(1o-base)(V)	−0.002	−.0.011	−0.011	−0.012	−0.004	−0.002	−0.010

9. SOLAR X-RAY DATA FROM THE GOES XRS

9.1 Sample Data From Large Solar X-Ray Flares

The solar x-ray data from the GOES XRS units are used by NOAA/NESDIS in its normal operations. The GOES solar x-ray data plots are published monthly in Solar Geophysical Data (U.S. Department of Commerce, Boulder, Colorado 80303). Fig. 9.1 is a plot of the GOES-5 solar x-ray flux for February 17 and 18, 1984, which includes a class X flare ($\geq 10^{-4}$ W/m^2 in the 1-8 A^{o} channel B flux) peaking near 2300 UT on the 17th. The plot in Fig. 9.1 is made from two one-day plots prepared by NOAA. The sun is quite active at this time, since the class X flare is preceded by a class M flare ($\geq 10^{-5}$ W/m^2 in channel B) at about 1200 UT on the 17th.

Details of the peak of the class X flare at 2300 UT are shown in Fig. 9.2, which is made from parts of three one-hour plots prepared by NOAA. The "spikes" shown in the plot are the range change transients, since the plot shows all XRS measurements, which are received every 3.06 second minor frame time. A detailed plot of each channel B measurement for the R2/R3 range change during the event rise is given in Fig. 9.3 to illustrate the 3 second time constant during the recovery following the range change. The fluxes plotted in Fig. 9.3 have been calculated from the telemetry voltage using the sensor temperature (23.1^{o}C) and the temperature-corrected calibration constants from Table 7.2. The NOAA-calculated fluxes in Figs. 9.1 and 9.2 are about 8% lower using adjusted 25°C calibration constants to bring agreement with the earlier SMS-2 XRS data (see Sections 9.2 and 11.3).

During February 1984 the GOES-5 XRS sensor was at about 23°C and the GOES-6 sensor at about 20°C (the electronic units (DPUs) were about 18°C and 15°C, respectively). The sensor temperatures are near the yearly maximum (earth orbit perihelion is near January 3), and are close to the calibration base temperature of 25°C. Temperature corrections to the calibration constants are thus small for these data.

Similar x-ray flux plots can be obtained for other solar x-ray flares, as most of the GOES-5/GOES-6 x-ray data are archived at NOAA/NESDIS. The x-ray fluxes have been normalized to the SMS-2 fluxes, which were originally used as a base for the GOES XRS fluxes (Ref. 16).

9.2 Intercomparison of the GOES XRS Units

The GOES-4, 5 and 6 XRS solar x-ray fluxes have been compared in-orbit with each other and with GOES-2. The GOES-2 x-ray fluxes form the basis for the normalization to the SMS-2 base. The GOES-2 x-ray calibration constants as originally specified are obtained from Ref. 17, and listed in Table 9.1. These values were used for the comparisons with GOES-4 and GOES-5. The actual working calibration constants for GOES-2 were obtained from NOAA/ERL (Ref. 18), and are also listed in Table 9.1. The Ref. 18 values are adjusted to have the GOES-2 x-ray fluxes agree
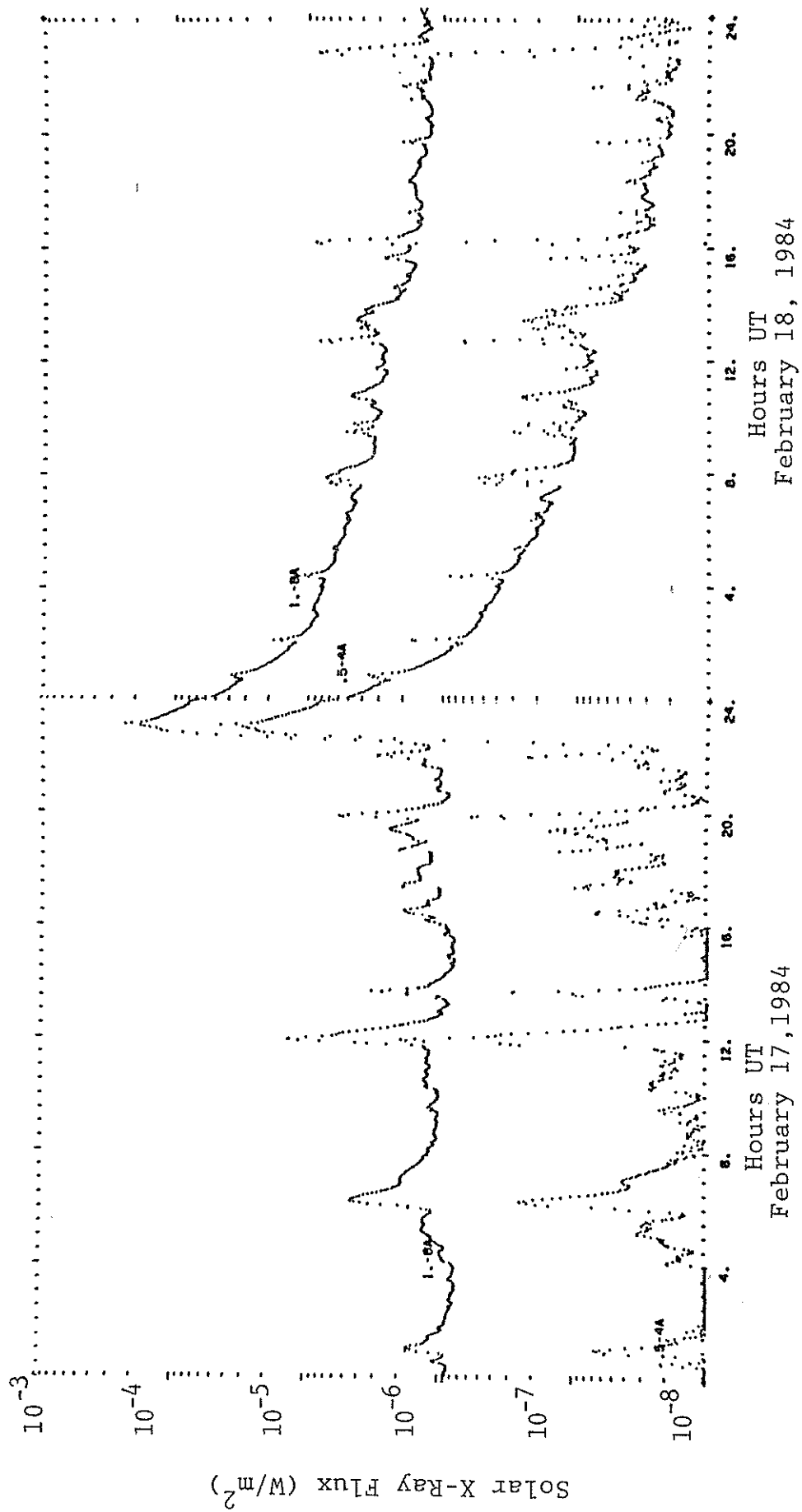
Figure 9.1. GOES-5 Solar X-Ray Flux for the February 17-18, 1984, Class X Flare.
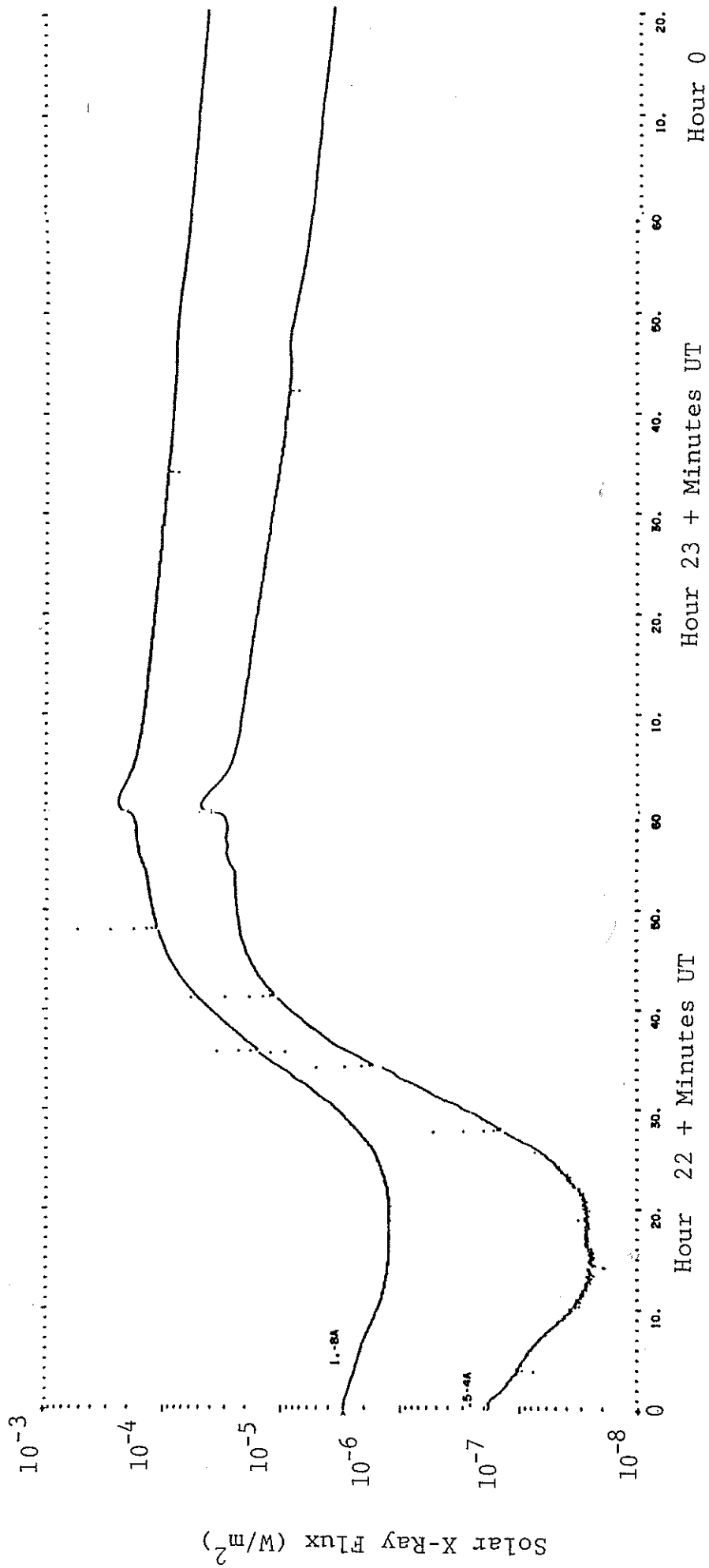
Figure 9.2. Details of the Solar X-Ray Flux Peak for the February 17-18, 1984 Class X Flare.
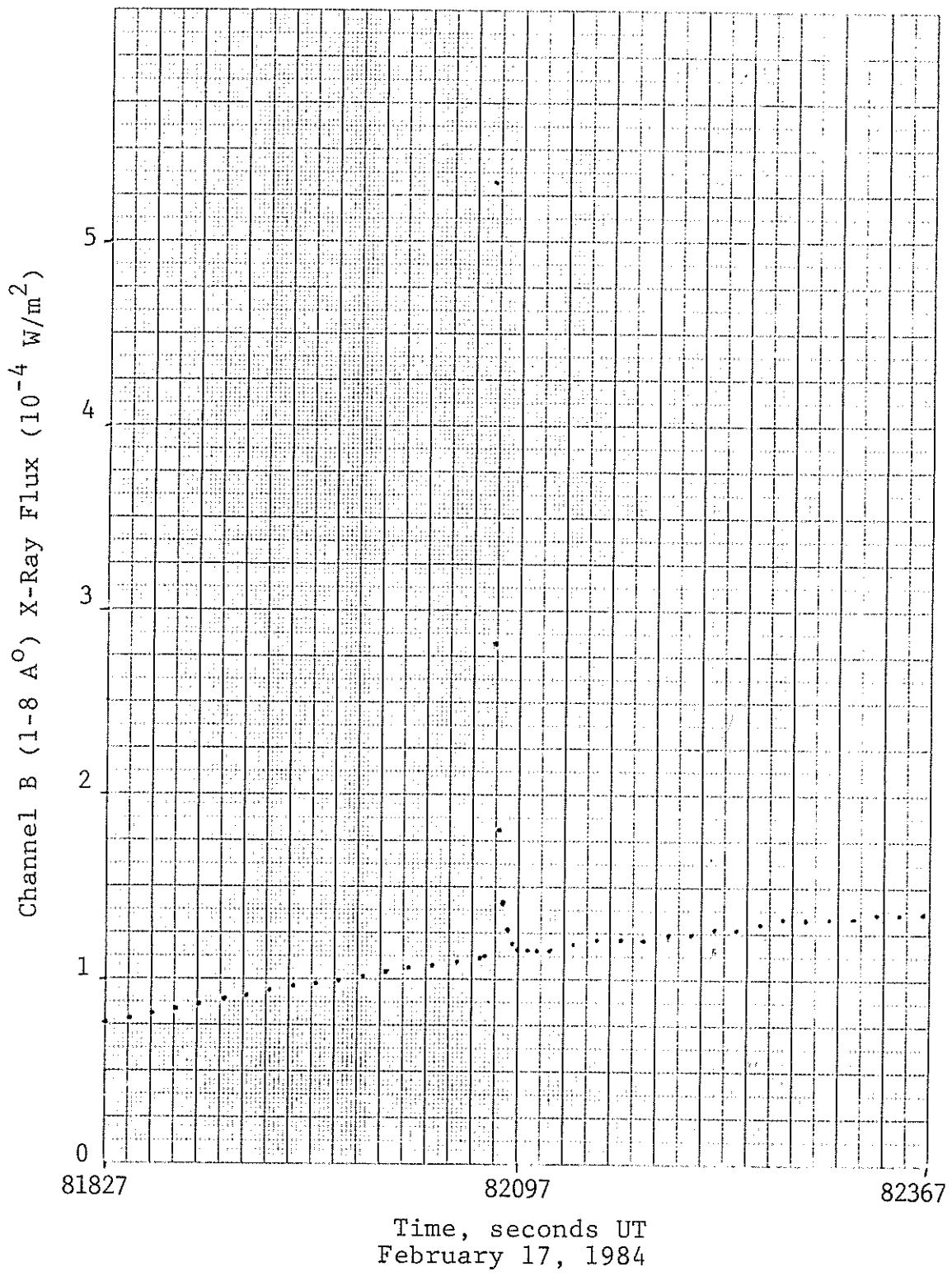
Figure 9.3.   GOES-5 Channel B X-Ray Fluxes at a Range
                Change (R2/R3), Showing the Response Time
                Constant.

96

with SMS-2, using the factors listed at the bottom of Table 9.1. The channel B factor of 1.089 differs slightly from the 1.098 factor given on p. 18 of Ref. 16, but the < 1% difference is not significant.

The telemetry data print-outs for GOES-2, 4, 5 and 6 were used to compare the x-ray responses for a number of solar flares

Table 9.1

GOES-2 XRS Calibration Constants

$$\text{x-ray flux} = (\text{TM volts} - V_o) \times S_x \text{ (Range)}$$
$$V_o = \text{offset in volts}$$
$$S_x = \text{calibration constant to give W/m}^2 \text{ x-ray flux}$$

Channel/Range	$V_o(V)$	S_x (Ref. 71)	S_x (Ref. 18)*
A/R3	0.60	3.417×10^{-5}	4.005×10^{-5}
A/R2	0.60	3.324×10^{-6}	3.896×10^{-6}
A/R1	0.60	3.373×10^{-7}	3.953×10^{-7}
A/R0	0.60	3.431×10^{-8}	4.021×10^{-8}
B/R3	0.59	3.193×10^{-4}	3.476×10^{-4}
B/R2	0.59	3.134×10^{-5}	3.412×10^{-5}
B/R1	0.59	3.313×10^{-6}	3.607×10^{-6}
B/R0	0.59	3.369×10^{-7}	3.668×10^{-7}

---

*These are the values of S_x used by NOAA for calculating the GOES-2 solar x-ray fluxes. The channel A values are larger by 1.172, and the channel B values are larger by 1.089.

where data from two spacecraft was available. The resulting measured flux ratios, using the 25°C calibration constants, are listed in Table 9.2 for the four ranges (where obtainable) of each x-ray channel. The listed ratios are averages for each range, over a number of events, and are accurate to about ± 3%. The A channel R1 and R0 ranges for GOES-2 show anomalous behavior, with widely varying ratios for both GOES-4 and GOES-5 comparisons, so the listed values are only estimates (GOES-5/GOES-4 A channel R1 and R0 values are quite stable, so the variation is in GOES-2).

The XRS units also show step changes in x-ray flux at the range changes because of slight differences in the calibration for different ranges. The step change for the GOES-4 B channel is shown in the plot of Fig. 9.4 for the R2/R1 range change. This method of obtaining the range change steps only works for a smoothly changing solar x-ray flux as shown in Fig. 9.4. Another method of obtaining the range change steps is to compare the flux ratios of two XRS units where the range changes occur at different flux levels. This allows one XRS unit to provide a flux normalization for the unit having the range change, and will work for both units in turn. The measured range change steps are listed in Table 9.3 for GOES-2, 4, 5 and 6. The data are averages for several solar x-ray flares and are accurate to about ± 3%.

The normalized x-ray flux ratios from the direct measurements in Table 9.2 and from the range change steps in Table 9.3 are compared in Table 9.4. The two sets of ratios agree to within 5% except for the A channel R1, R0 ratios involving GOES-2, where the measurements have a large uncertainty because of the GOES-2 flux variations. Note that in all cases the (R3, R2) and (R1, R0) flux ratios are equal to within 5%, so the major variations with range come primarily from the factor 100 gain change in the preamplifier which occurs at the R2/R1 range switch.

The correction factors to normalize the measured x-ray fluxes to the SMS-2 equivalent fluxes are listed in Table 9.5. The GOES-2 values are taken from Ref. 18 and the other ratios are calculated from the average of the ratios in Table 9.2. The x-ray fluxes calculated from the pre-launch calibration constants should be multiplied by the factors in Table 9.2. The correction factors are estimated to be accurate to ± 5% because of the multiple transfers involved, particularly for GOES-6. The average value for the A channel shows that all four XRS units give a flux about 25% lower than the SMS-2 XRS, while the B channels are about the same as for SMS-2. The variations among the GOES-2, 4, 5 and 6 XRS units is about ± 10% for channel A and ± 13% for channel B.

Table 9.2

Measured X-Ray Flux Ratios for GOES-2, 4, 5 and 6 XRS Units

| Channel/Range | Measured ratios for (GOES-a)/(GOES-b) | | | |
	4/2	5/2	5/4	6/5
A/R3	0.85	0.94	--	0.87
A/R2	0.86	0.96	1.14	0.85
A/R1	~ 0.95	--	1.04	0.88
A/R0	~ 0.99	--	1.04	0.88
B/R3	1.07	1.01	--	1.16
B/R2	1.07	1.01	1.00	1.15
B/R1	1.13	--	1.02	1.16
B/R0	1.11	--	--	1.16

Table 9.3

X-Ray Flux Ratios for Adjacent Range for GOES-2, 4, 5 and 6

| Channel /(Range Ratio) | Flux (high range)/Flux (low range) for | | | |
	GOES-2	GOES-4	GOES-5	GOES-6
A/(R3/R2)	1.00	1.00	1.03	1.04
A/(R2/R1)	1.00	0.96	1.09	1.06
A/(R1/R0)	~ 1.00	1.00	0.95	0.96
B/(R3/R2)	0.99	1.01	1.03	1.04
B/(R2/R1)	0.98	0.93	0.95	0.94
B/(R1/R0)	0.96	1.00	1.01	1.01

GOES-4 R2/R1 range change

Flux ratio (25°C Cals): $\dfrac{R2}{R1} = \dfrac{9.19}{10.01} = 0.92$
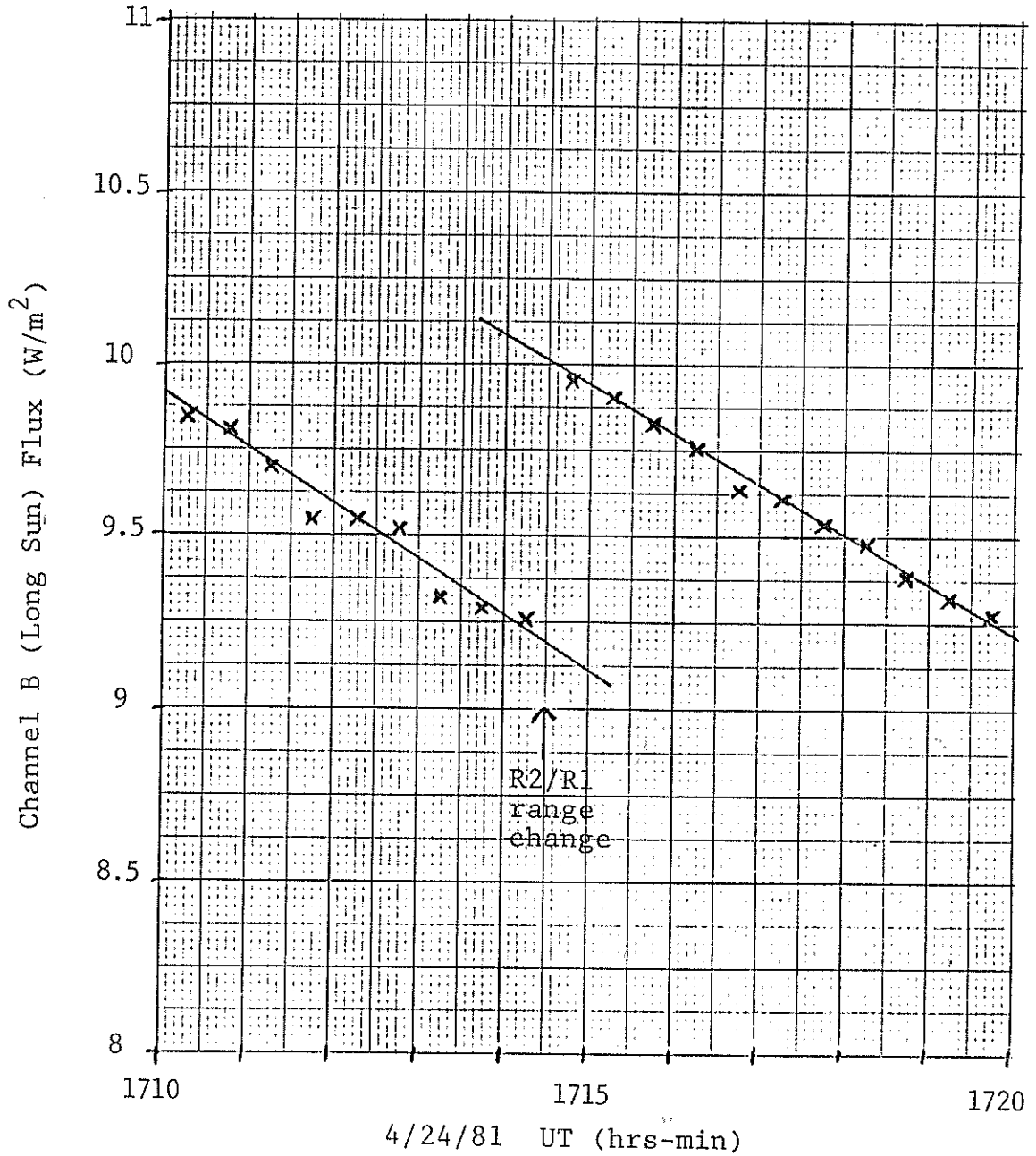
Figure 9.4. Plot Showing Flux Step Change at R2/R1 Range Change for GOES-4 B Channel.

Table 9.4

Normalized X-Ray Flux Ratios for GOES-2, 4, 5 and 6

Channel /Range	(G-4)/(G-2) Meas.	(G-4)/(G-2) Calc.	(G-5)/(G-2) Meas.	(G-5)/(G-2) Calc.	(G-5)/(G-4) Meas.	(G-5)/(G-4) Calc.	(G-6)/(G-5) Meas.	(G-6)/(G-5) Calc.
A/R3	≌1.00	≌1.00	≌1.00	≌1.00	--	1.11	≌1.00	≌1.00
A/R2	1.01	1.00	1.02	0.97	1.10	1.08	0.98	0.99
A/R1	~1.12	1.04	--	0.89	1.00	0.95	1.01	1.02
A/R0	~1.16	~1.04	--	~0.94	≌1.00	≌1.00	1.01	1.01
B/R3	≌1.00	≌1.00	≌1.00	≌1.00	--	1.02	≌1.00	≌1.00
B/R2	1.00	0.98	1.00	0.96	≌1.00	≌1.00	0.99	0.99
B/R1	1.06	1.03	--	0.99	1.02	0.98	1.00	1.00
B/R0	1.04	0.99	--	0.94	--	0.97	1.00	1.00

Note: <u>Meas.</u> values are from the direct flux ratio data in Table 9.2

<u>Calc.</u> values are from the range change steps ratios in Table 9.3.

Table 9.5

Correction Factors to Normalize GOES-2, 4, 5 and 6 X-Ray Fluxes to SMS-2

Channel/Range	G-2	G-4	G-5	G-6	Average
A/(R3, R2)	1.172	1.36	1.23	1.43	1.30
A/(R1, R0)	1.172	1.21	1.16	1.32	1.22
B/(R3, R2)	1.089	1.02	1.08	0.93	1.03
B/(R1, R0)	1.089	0.97	0.96	0.83	0.96

Note: x-ray fluxes calculated from the pre-launch calibration constants should be mutliplied by the above factors to give the effective SMS-2 measured x-ray fluxes.

9.3 Long Term XRS Stability

The long term in-orbit stability of the GOES XRS units depends on stable electronics and ion chambers. The electronics stability can be verified by the IFC data, and as shown in Section 8.3 is generally stable to 1%, with some possible 3% shifts in the highest gain channels. The IFC does not verify the ion chamber response, where small gas leaks could result in a slow decrease in x-ray response. The in-orbit comparison of the GOES-2, 4, 5 and 6 XRS units discussed in Section 9.2 shows that the A channels are equal to $\pm$ 10% and the B channels to $\pm$13%. These data show that at least up to late 1982/early 1983 the GOES-2 XRS ion chambers had not leaked to about a 10% limit, and that the GOES-4, 5 and 6 ion chambers had all survived launch and initial operation for 1-2 years with about a 10% limit on the possible gas leaks.

In June, 1986 the XRS on GOES-4 was turned on for about 2 weeks, and this allowed intercomparison of GOES-4, 5 and 6 x-ray sensors after GOES-4 was in orbit for 5.75 years. The GOES-4 XRS was not properly synchronized to the solar direction, but was synchronized to the earth horizon and so measured actual solar x-rays only once per day near 0200 UT. On June 14, 1986, there was a weak solar x-ray flare which gave useful fluxes only in channel B/R0, but peaked near 0200 UT. As the GOES-2 XRS phasing passed through the sun it was possible to measure the relative B/R0 responses of GOES-4, 5 and 6. The measured ratios are

$$\frac{(G-5)}{(G-4)} \ (B/R0) = 1.05 \qquad (6/14/86)$$

$$\frac{(G-6)}{(G-5)} \ (B/R0) = 1.17 \qquad (6/14/86)$$

The (G-6)/(G-5) ratio is within 1% of the earlier measured ratio, while the September 10, 1981 data for (G-5)/(G-4) from Tables 9.2 and 9.3 can be used to derive a value of

$$\frac{(G-5)}{(G-4)} \ (B/R0) = 1.01 \qquad (9/10/81)$$

Thus, if we assume the (G-5)(B/R0) response is stable, then the (G-4)(B/R0) response has decreased by about 4% in 4.75 years. This is about the measurement accuracy, allowing for pointing errors and the comparatively low peak flux of about 10^{-7} W/m^2. The data show that the GOES-4 XRS B channel ion chamber has not leaked to less than 5% gas loss, and the data are consistent with less than 1% gas loss over 5.75 years.

The above data could be explained by all three B chambers leaking at the same rate, but this is extremely unlikely. The most tenable conclusion is that all three B chambers have leaked

less than a few % of their gas content in the 5.75 to 3.1 years they had been in orbit as of June 1986.

The A channel fluxes were very weak, near 10^{-9} W/m^2, and were strongly affected by small shifts in the offset voltage. All three XRS units agree to at least 50% at the event peak, so the A chambers have not experienced any large leaks.

All ion chambers for GOES-4 through H, plus spares, were stability/leak tested at Panametrics for several months to 2 years in a test fixture using Fe-55 x-ray sources in vacuum. The results for the GOES-4, 5 and 6 ion chambers are shown in Table 9.6, while the GOES-G, H, spares and the original Keithley Engineering Model XRS ion chamber data are shown in Table 9.7. The results in Table 9.6 show an ion chamber response increase of about 5% over the first several months, which appears to stabilize. This is just at the limit of the 4% accuracy on the calibration of the electrometer used to make the ion chamber current measurements. The data in Table 9.7 indicate about a 6% increase in the B chamber response, which may be significant since the Keithley EM ion chamber is stable to 1%. The data in Tables 9.6 and 9.7 are consistent with an increase in A chamber response of about 2 to 6% and B chamber response of 4 to 11%. most of this increase occurring over the first year following manufacture. Following this initial increase, the ion chambers appear to have long-term stability near 1%.

The 5-10% increase in ion chamber response may possibly be due to "aging" of the Xe (0.5% He) and Ar (0.5% He) fill gases, where trace contaminants achieve a final equilibrium concentration. The final trace gas concentration could be higher (outgassing from the walls, etc.) or lower (gathering of reactive gases by wall and/or other materials inside the ion chamber). According to Ref. 19, pp. 31-35, Ar has an electron mobility which is strongly dependent on trace gas concentrations, while Ref. 20, p. 8-38 indicates that the W (eV/electron-ion pair) value for He is strongly dependent on trace gas concentration. These gas properties may account for the observed ion chamber response changes during the first year following fill, but this is only a plausible hypothesis and would require extensive testing to verify.

Since the gain increase is only about 5-10%, and appears to be stable to 1% or so after about 1 year of aging, it is not a critical factor. The only practical requirement is that detailed ion chambers calibration should be done after 1/2 to 1 year of aging to avoid a possible in-orbit gain increase above the XRS calibration. Since the calibration accuracy is typically about 10% (A chamber) to 15% (B chamber) (Refs. 14, 15), the "aging" gain increase of 5-10% will generally not be readily noticed from in-orbit data, although it may account for part of the observed differences between in-orbit XRS responses (e.g., the 16% difference of the GOES-5 and GOES-6 B channel - see Table 9.2).

Once the ion chambers have "aged" for 1/2 - 1 year, the absolute x-ray calibration appears to be stable to 1%, and in-orbit data indicate that long-term ion chamber stability is likely to be better than 5%.

Table 9.6

GOES-4, 5 and 6 Ion Chamber Stability Test Results

| Date of test | Stability test results for ion chamber | | | | | | | |
| | SN W2337 | | GOES-4 SN W2338 | | GOES-6 SN W2339 | | GOES-5 SN W2340 | |
	A	B	A	B	A	B	A	B
9/78 (base)	1.00	1.00	1.00	1.00	1.00	1.00	1.00	1.00
1/79			1.02	1.01				
5/79	1.04	1.02	1.06	1.04	1.05	1.04	1.06	1.07
11/79					1.03	1.04	1.04	1.04
6/80	1.07	1.07	1.06	1.03				
Average of last 2	1.06	1.05	1.06	1.03	1.04	1.04	1.05	1.06

Final average for A chambers = 1.05

Final average for B chambers = 1.04

Note: Engineering Model Ion Chamber   SN W2336 from 6/78 to 9/78
        showed response changes of:

                A chamber = 1.06
                B chamber = 1.11

Table 9.7

GOES-G, H Ion Chamber Stability Test Results

Date of test	GOES-G SN B1652		SN B1653		SN B1654		GOES-H SN B1655		Keithley Eng. Mod.	
	A	B	A	B	A	B	A	B	A	B
1/84 (based)	1.00	1.00	1.00	1.00	1.00	1.00	1.00	1.00	1.00	1.00
2/84	1.01	0.99	1.00	0.99	1.00	1.00	1.01	1.01	1.00	1.01
6/84	1.01	1.05	1.02	1.04	1.01	1.08	1.01	1.05	1.00	1.01
10/86					1.04	1.11				

Stability test results for ion chamber

6/84 Average for A chambers (four) = 1.02/Keithley EM = 1.00

6/84 Average for B chambers (four) = 1.06/Keithley EM = 1.01

10. COMPARISON OF XRS BACKGROUND AND EPS ELECTRON DATA

The XRS narrow band (NB) background channel gives the average ion chamber current. The average current normally consists of two components: the averaged current from the solar x-ray pulse (100/sec at about a 10% duty cycle); and the electron induced background current. During solar proton events there are also currents from the higher energy protons (above about 7.9 MeV for channel A and 2.3 MeV for channel B). The XRS NB background channel response to x-rays can be calculated from the calibration data in Tables 7.2 and 7.3, using a 10% duty cycle for the solar x-ray pulse based on the 36° FWHM of the XRS telescope FOV in the sweep direction. The NB response can also be measured in-orbit during periods of varying x-ray flux, but low, constant particle (electron - E1) fluxes.

Figures 10.1 and 10.2 show measured NB vs. x-ray flux responses for the GOES-5 XRS during a 10/7-8/81 x-ray event. The data are for R1 and R2, and are for a period of low E1 counts (about 1/sec or less) during the rising part of the x-ray event. The measured NB/x-ray flux slopes in Figs. 10.1 and 10.2 are compared with a number of other measurements in Table 10.1, and the average measured response is compared with the calibrated response at 10% duty cycle. The agreement is quite good and shows that the x-ray contribution to the NB background current can be readily calculated from the calibration constants. Some GOES-6 XRS NB data for the 5/27-28/83 event are in good agreement with the GOES-5 data, so all XRS units can be readily corrected for x-ray flux contribution to the NB background current.

Channel A corrected NB background current for the GOES-5 XRS is plotted against the EPS E1 countrate in Fig. 10.3. The NB current is corrected for x-ray flux effects by

$$I_{NB} \text{ (corr.)} = I_{NB} - 1.79 \times 10^{-6} J_x \qquad (10.1)$$

where I_{NB} in A is calculated from (7.4) and J_x in W/m^2 is calculated from (7.1). The data in Fig. 10.3 are for a high electron flux period in 10/85, and are fit to $\pm$ 30% by a straight line of slope 7.8×10^{-17} A/(el/readout). At low electron fluxes the 10/10-11/85 data show some large deviations from the higher flux fit, and this is shown better in Fig. 10.4 where a number of sets of low electron flux data are shown. The slope in Fig. 10.4 is 8.5×10^{-16} A/(el/readout), about ten times the slope in Fig. 10.3. The XRS response to electron background, based only on the E1 (> 2 MeV) electron flux, thus has at least two different response types. Note that proton flux effects are also observed as shown by the 11/25-26/82 data in Fig. 10.4, where the same E1 slope is observed, but with an offset of about 2.7×10^{-13} A.

The channel B corrected NB background currents are plotted in Fig. 10.5 for high electron fluxes and Fig. 10.6 for low electron fluxes. The corrections were made with (10.1) but using a correction factor of 4.8×10^{-7} A-m^2/W, based primarily on the Figure 10.1

GOES-5, XRS A Channel
Narrow band background
vs. Solar x-ray flux.
R1/R2 data, 10/7-8/81

1.55×10^{-6} A-m^2/W
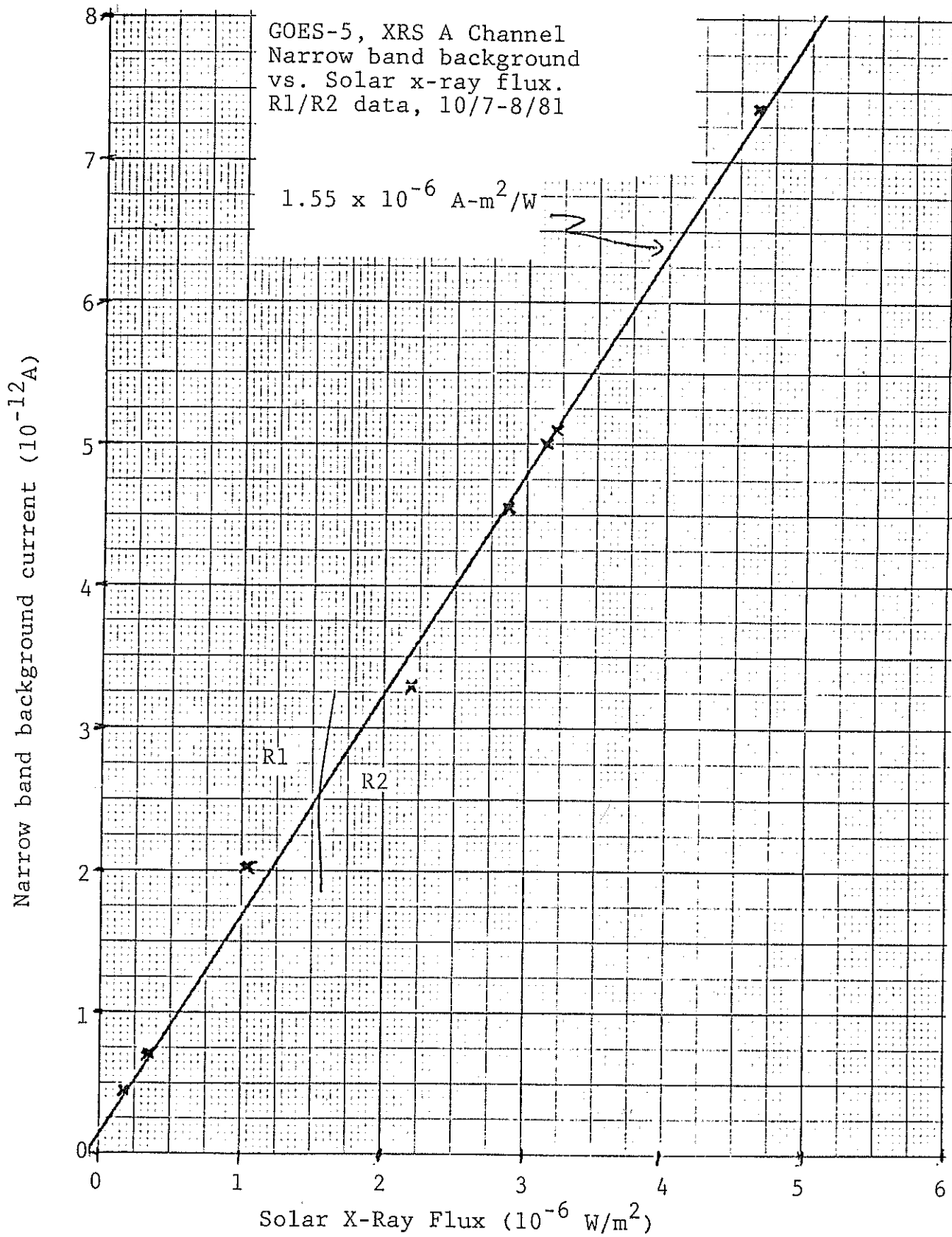
Figure 10.1. GOES-5 XRS Channel A NB Background
vs. Solar X-Ray Flux
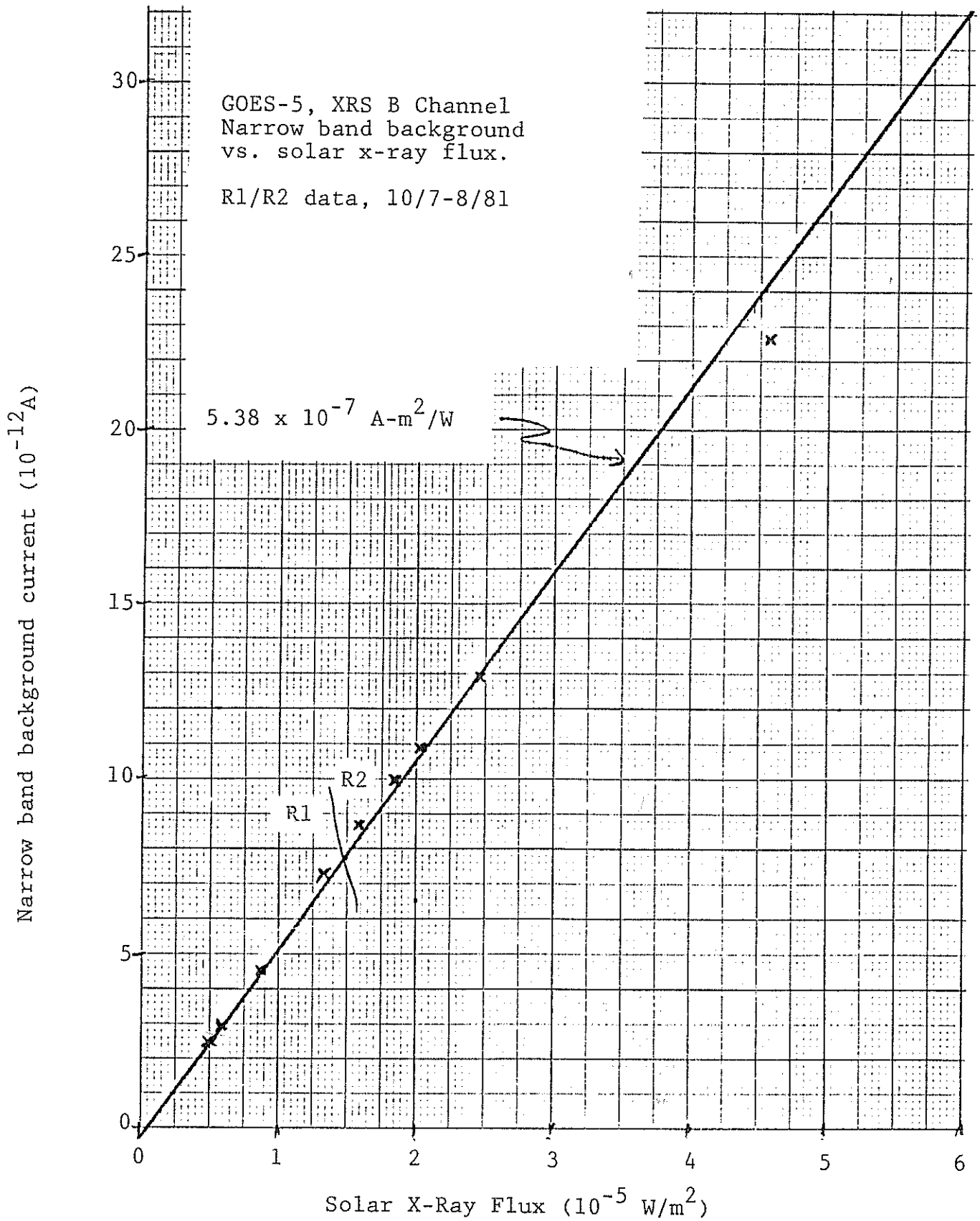
Figure 10.2.   GOES-5 XRS Channel B NB Background
vs. Solar X-Ray Flux

Table 10.1

GOES-5 XRS NB Background Response to X-Rays

Date of data	XRS Ranges used	X-Ray Event condition	NB response $(A-m^2/W)$	
			Channel A	Channel B
10/7-8/81	R2/R1	Event rise	1.55×10^{-6}	5.38×10^{-7}
10/7-8/81	R2	Event fall	1.68×10^{-6}	4.93×10^{-7}
10/7-8/81	R1	Event fall	1.81×10^{-6}	4.63×10^{-7}
6/4/81	R1/R0	Weak event; low E1 counts	1.89×10^{-6}	6.36×10^{-7}
5/27-28/83 and 7/19/81	R1/R0	Weak fluxes; low E1 counts	2.02×10^{-6}	4.76×10^{-7}
		Average (5) =	1.79×10^{-6}	5.21×10^{-7}
	Calibration K/10 (Table 7.2) =		1.74×10^{-6}	4.84×10^{-7}
		Measured/Calibration =	1.03	1.08

Figure 10.3. GOES-5 Channel A Corrected Background Current
vs. El Count Rate for High Electron Fluxes

The figure shows a plot titled "GOES-5 Corrected NB current vs. El count rate" with the following annotations:

x – 10/10-11/85

– 10/8/85

High El flux slope $=7.8 \times 10^{-17}$ $\dfrac{A}{el/readout}$

Y-axis: El Counts/readout ($= 3.06$ sec.) (in 10^3 counts/readout)

X-axis: Corrected NB Background Current (10^{-13}A)

GOES-5 Channel A

GOES-5

x - 8/20/85 data
  - 2/1-2/85 data
  - 11/25-26/82 data,
with low E proton fluxes.
  - 7/17/81 data with
very low particle fluxes.
  - 8/1/83 data

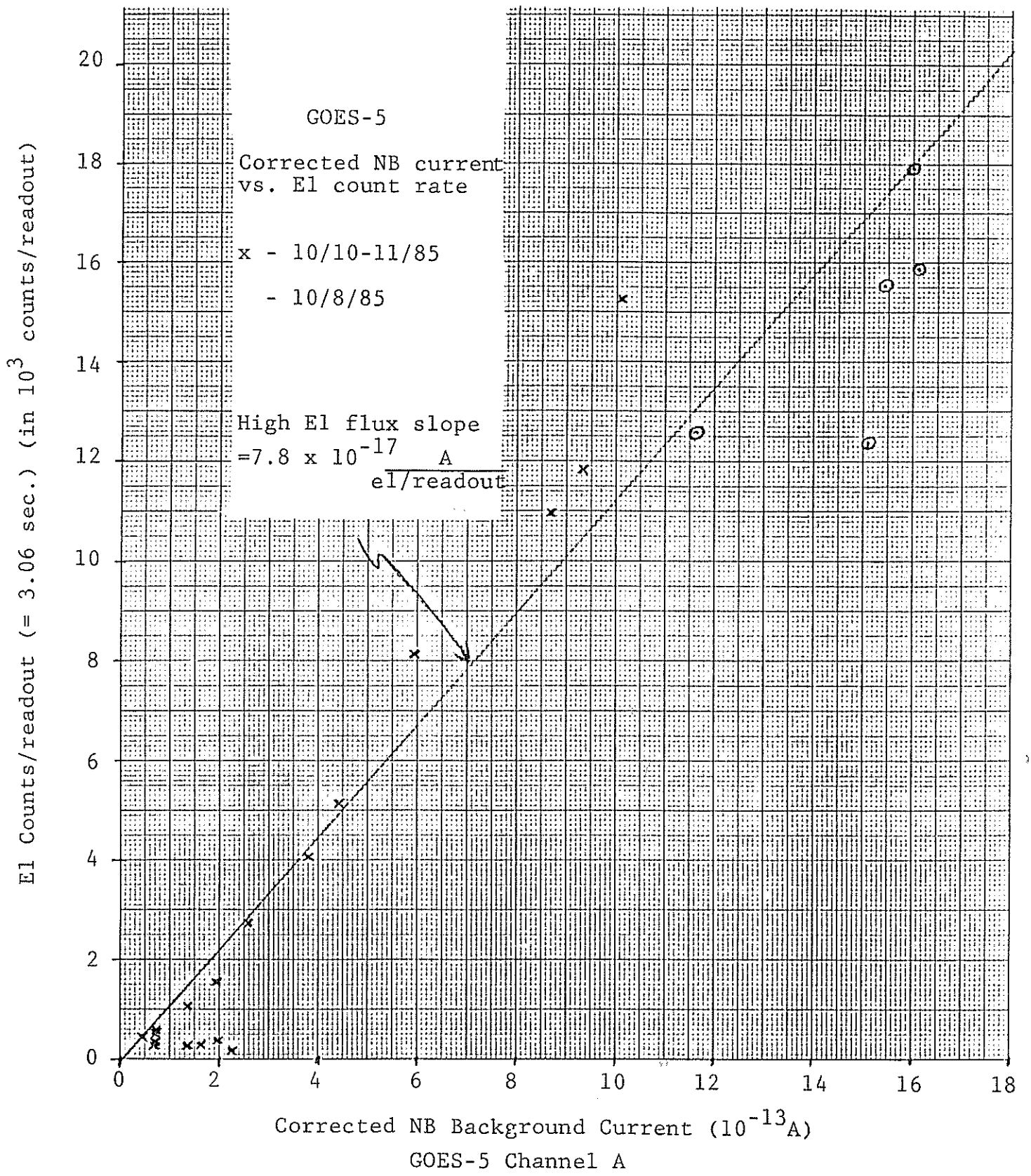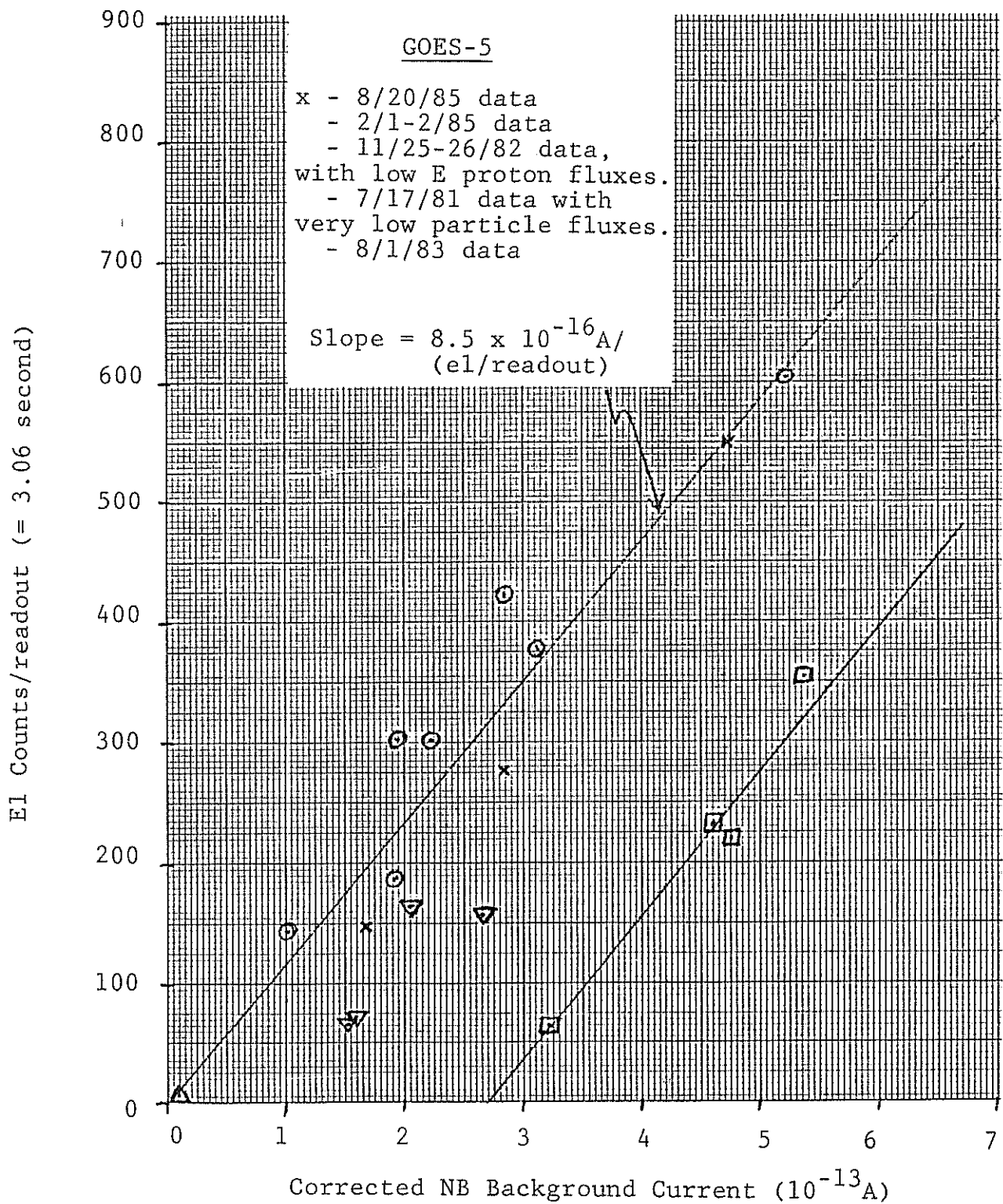Slope = 8.5×10^{-16}A/
(el/readout)

Figure 10.4.   GOES-5 Channel A Corrected NB Background
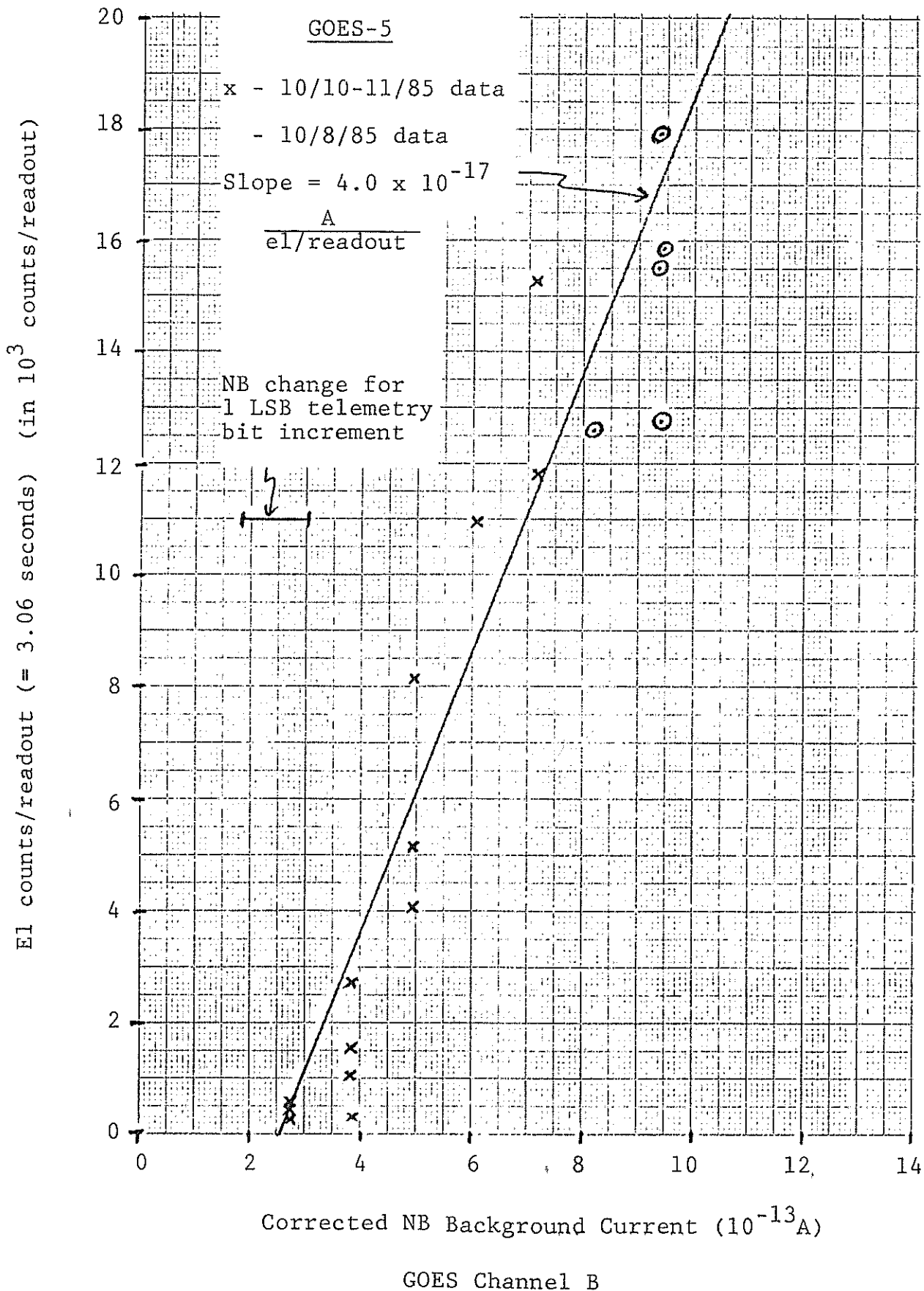Current vs. El Count Rate for Low Electron Fluxes

Figure 10.5. GOES-5 Channel B Corrected NB Background
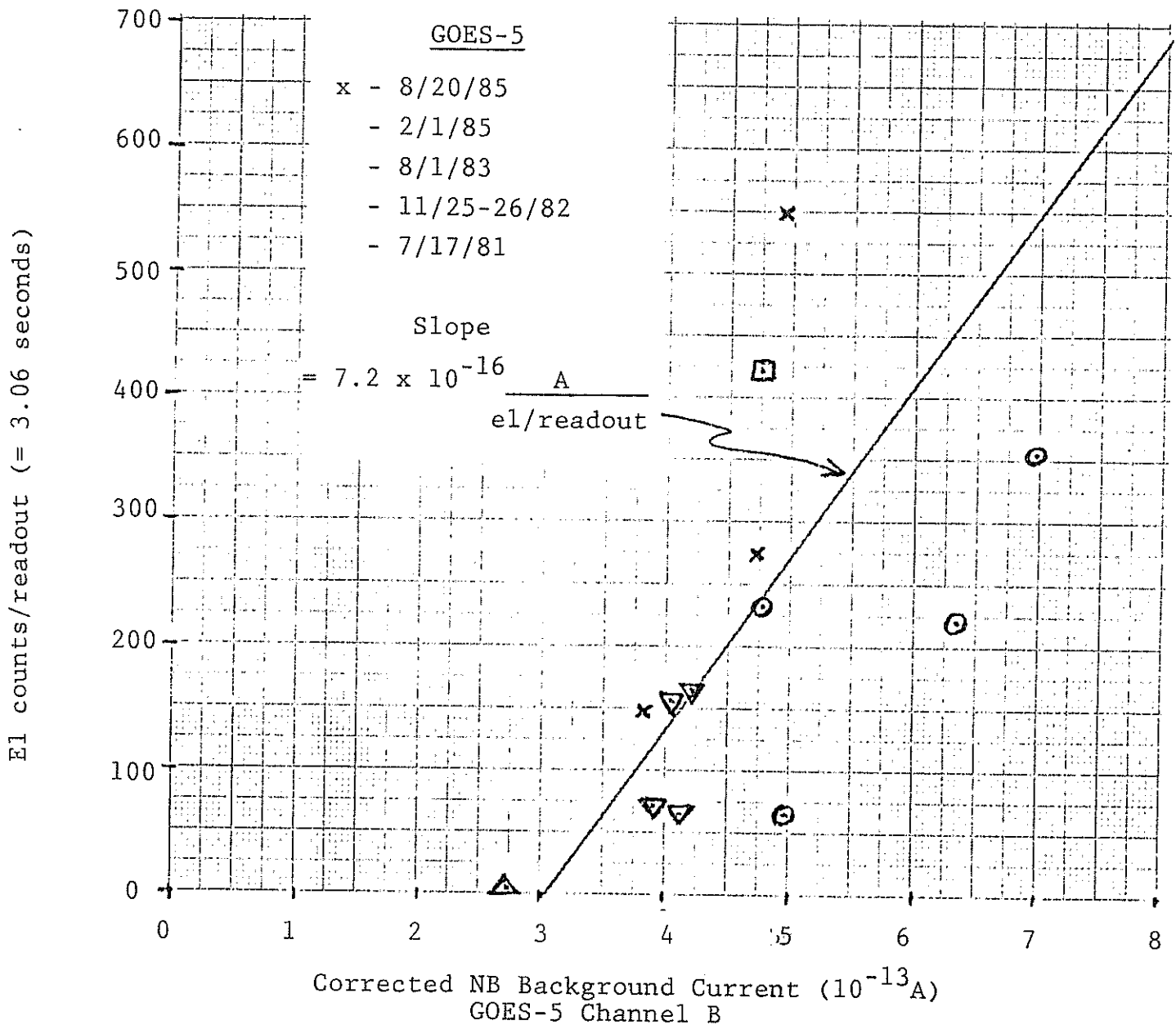Current vs. El Count Rate for High Electron Fluxes.

112

Figure 10.6. GOES-5 Channel B Corrected NB Background Current vs. E1 Count Rate for Low Electron Fluxes.

pre-launch calibration data. The channel B high/low electron fluxes show slopes about a factor of 20 different, slightly larger than for channel A. Note, however, that the channel B NB background signal is quite low, with 1 LSB telemetry bit increment giving the current change shown in Fig. 10.5 (x-ray flux corrections shift the NB current from exact 1 LSB bit positions), so the channel B data fits are less accurate, particularly at low El count rates.

The XRS response to electrons comes through two mechanisms: the direct irradiation by electron above about 2 MeV which are not deflected by the shielding magnet; and bremsstrahlung produced in the XRS housing and spacecraft, and which penetrate the ion chamber shielding to produce a current. The estimated responses for these two mechanisms are listed in Table 10.2, along with comparisons to the measured data.

The direct electron response (line 1 of Table 10.2) is obtained from the magnet shielding calculations in Ref. 21, and is normalized to the El geometric factor and count time (3.06 second) to give A/(el/readout). The direct response comes primarily from electrons above about 2 MeV, since the shielding magnet prevents lower energy electrons from reaching the ion chamber windows (see Ref. 21).

The bremsstrahlung response is calculated using the electron spectrum for GOES 160°W in Ref. 12, with bremsstrahlung production in Al. The bremsstrahlung are attenuated by Al (1.0 g/cm^2), Fe (1.1 g/cm^2 – the ion chamber wall), and Pb (1.8 g/cm^2), with PB attenuation for only half of the ion chamber solid angle since the ion chamber has Pb shielding on only part of the sides, top, and bottom. The transmitted bremsstrahlung are absorbed by the ion chamber gas (Xe or Ar). The precise calculation method, particularly for energy loss in the gas, is complex and will not be discussed in more detail. The results are listed in Table 10.2, and the response comes primarily from electrons below 1 MeV. The calculated bremsstrahlung repsonse vs. the El (> 2 MeV) electron count rate is thus strongly dependent on the spectral shape, and will not be correct for electron spectra significantly different from the GOES 160°W spectrum in Ref. 12. The calculated bremmstrahlung response is also uncertain because of the crude approximation of the spacecraft shielding by 1.0 g/cm^2 Al, so the calculated results in Table 10.2 are uncertain by at least a factor of 2.

The comparison of measurements and calculations in Table 10.2 lead to some interesting conclusions. For high electron fluxes the best agreement is with the direct electron irradiation calculation (line 4 vs. line 1), which suggests a harder electron spectra than the GOES 160°W model. The channel A calculation is in reasonable agreement with the in-orbit data, while the B channel calculation is about a factor of 5 high. For low electron fluxes the total electron calculation is in good agreement for channel A, but a factor of 2.5 low for channel B. The A channel data thus indicate that low electron fluxes are consistent with the GOES 160°W spectral shape of Ref. 12, with electron bremsstrahlung producing the dominant signal, while the high electron

114

Table 10.2

Estimated XRS Electron Responses and Comparison with Measurements

| Background Mechanism | Ion Chamber Responses – A(el/readout) | | Line Number |
	Channel A	Channel B	
Direct electron irrad. (Ref. 21)	1.02×10^{-16}	2.2×10^{-16}	1
Bremsstrahlung	8.6×10^{-16}	6.5×10^{-17}	2
Total electron response	9.3×10^{-16}	2.9×10^{-16}	3
Measured high flux (Ratio line 4/	7.8×10^{-17}	4.0×10^{-17}	4
line 1)	(0.76)	(0.18)	5
Measured low flux (Ratio line 6/	8.5×10^{-16}	7.2×10^{-16}	6
line 3)	(0.91)	(2.5)	7

fluxes are associated with harder electron spectra where the direct electron irradiation effect is dominant.

The channel B calculated responses are in poor agreement with the measurements. The high electron flux calculation can be improved by allowing for the angled incidence of electrons on the B chamber window, since most electrons have been deflected upward by the shielding magnet (see Fig. 7.3 and Ref. 21). The Be UV shield is located about 0.45 inch in front of the ion chamber window, and the 0.050 inch thick, 0.096 inch wide support bar between the A and B chamber apertures would thus shield the B chamber window from electrons at incident angles between 10° and 30°. The support bar is equal to the range of a 1.6 MeV electron, so even high energy electrons would be scattered out of the direction of the B window. Maximum shielding would be a factor of 0.62 in response, so allowing for some electron penetration would suggest a factor of about 0.75 for this shielding.

The angled electron incidence also results in only a fraction of the B chamber volume being irradiated by electrons. For incident angles (to the window normal) of 10° to 30° the geometrically irradiated volume fraction is 0.45 to 0.14. A reasonable average volume fraction would thus be 1/3, for a total correction factor of 0.25. This gives a corrected direct electron response calculation of 5.5×10^{-17} Al(el/readout), and a measured/calculated) response ratio of 0.73 for the high electron flux case. The total calculated response becomes 1.20×10^{-16} A/(el/readout), with a (measured/calculated) response ratio of 6.0 for the low flux case.

The B chamber calculations can thus be reasonably well corrected to agree with the high flux data, but the low flux data would require a bremsstrahlung response about 10 times the calculated value. One factor may be low energy proton contamination, since the B chamber 2 mil Be window (plus the 0.4 mil Be UV shield) allows protons above 2.3 MeV to reach the Ar fill gas. An approximate calculation assuming that 1/6 of the P1 (0.6 – 4.2 MeV protons) counts are for protons above 2.3 MeV gives a channel B NB current response of 1.0×10^{-15} A/(P1/readout), which is the same magnitude as the slope for electrons in Fig. 10.6. The B chamber low electron flux data are thus protentially contaminated by proton fluxes. Since the P1 counts are usually from low energy protons (< 2.3 MeV), the actual separation of E1/P1 effects is likely to be difficult. Note that the data in Figs. 10.5 and 10.6 show an offset of 3×10^{-13} A, which may be from protons. It should be noted that even at the times of very high electron flux, the P1 count was not significantly higher compared with the low electron flux periods, for both GOES-5 and GOES-6.

The high E1 electron fluxes on GOES-5 and GOES-6 correlate not only with the XRS background NB currents, but also with the HEPAD S1 count. The HEPAD S1 output is a 0.125 MeV threshold on the front solid state detector, and is thus sensitive to bremsstrahlung from electron above this energy. Early data from GOES-5 and GOES-6 are shown in Fig. 10.7, where both give approximately the same relation between E1 and S1. Figures 10.8 shows early and later data from GOES-6, illustrating the decreased
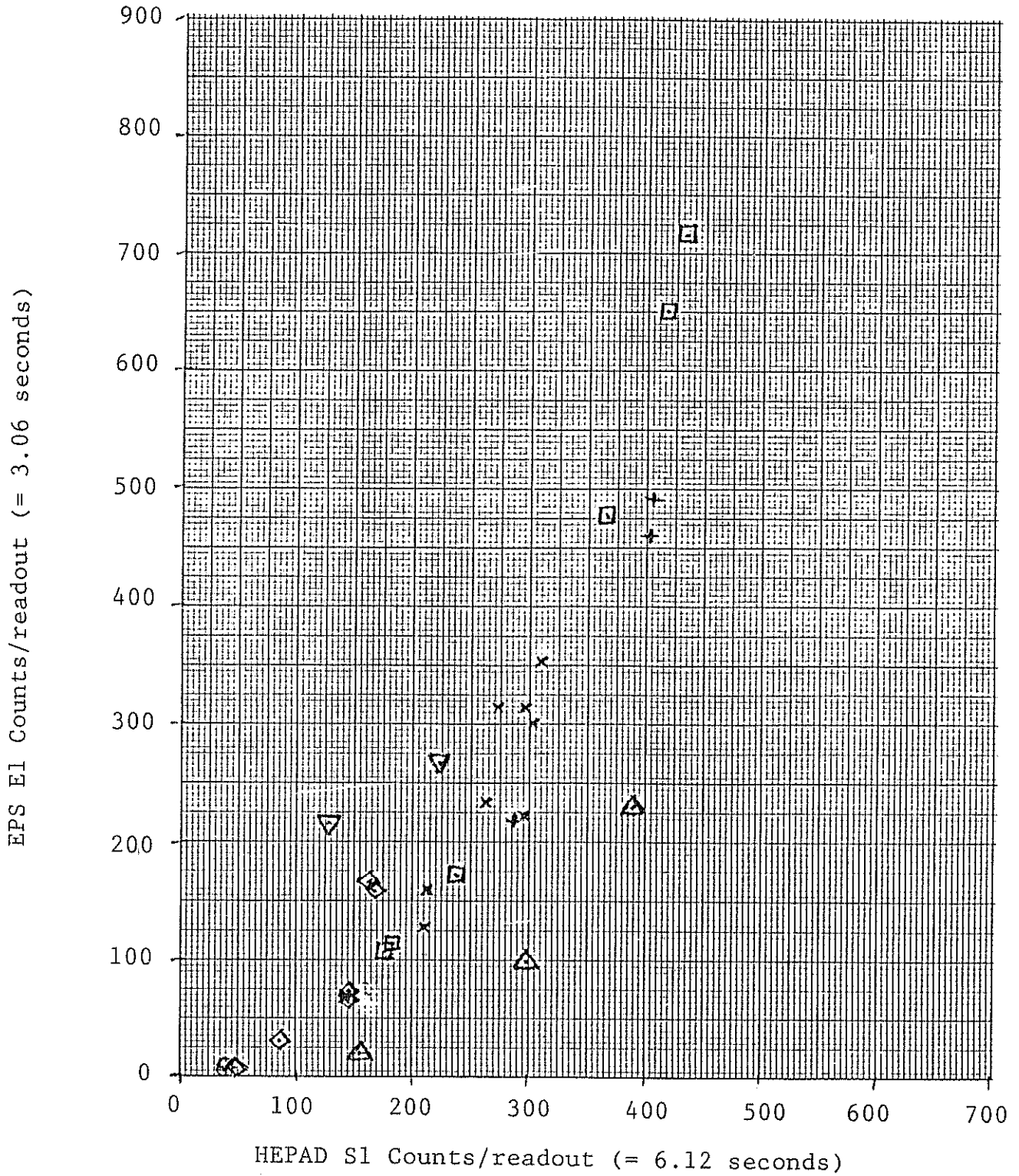
116

Figure 10.7.   GOES-5 and GOES-6 EPS E1 vs. HEPAD S1 Count Rates.

detection efficiently for the E1 channel with a partially depleted detector. From 5/83 to 10/85 the E1 channel detection efficiency on GOES-6 has dropped by a factor of about 4. A similar relation is found for the EPS E1 vs. HEPAD S3 count rates, but it is less obvious because of the large alpha lamp background.

The XRS background currents vs. EPS E1 electron count rate are in reasonable agreement with calculations, particularly for the A channel. The data indicate a change in electron spectral shape, with a harder spectrum at high E1 flux intensities. The B channel data indicate a possible proton flux contamination at low E1 count rates.

Figure 10.8.   GOES-6 EPS E1 vs. HEPAD S1 Count Rates.

11.   IN-ORBIT OPERATION OF THE GOES XRS

11.1 Routine IFC Operation

The GOES XRS units are generally put into the IFC mode for several minutes once per week.   The weekly IFC data should be checked for the ("hi"-"lo") values and the "lo" values, as discussed in Section 8.2   The acceptable "lo" values, are only for the upper ranges as determined by the pre-IFC solar x-ray flux, which should be < 0.75 V in the range in question, or < 3 V in the next lower range.   IFC data with a large E1 count rate may also be suspect.   If any of the "lo" values for the lowest ranges have shifted more than $\pm$ 5% with no solar x-ray flux effect, then the data should not be considered significant if E1 is large (> 1000 counts/readout is a good starting choice).

High proton fluxes can also affect the IFC data much like high electron fluxes.   A safe approach would be to ignore any "lo" deviations of more than $\pm$ 5% if the EPS P2 count is greater than 10/readout, or if the P4 count is greater than 100/readout. Particle or x-ray fluxes which are strong enough to saturate any of the "hi" values at 5.11 V, or the "lo" value at 0.00 V, will also give incorrect ("hi"-"lo") gain values.   Any significant changes of more than $\pm$ 5% should be verified for at least two IFC cycles a week apart and possible temperature effects should also be checked, before an anomaly in the IFC is noted.

The IFC "lo" values from all acceptable ranges should be averaged to give an effective base value for each XRS channel. The averaged IFC base values should be used for the x-ray flux calculation in (7.1) if the new IFC base differs from the current use base by more than 2% (2% is about one LSB increment in the telemetry signal).   Note that if temperature corrections are used for (7.1), then the IFC base should be corrected to 25°C using the DC_x values of (7.2) to generate a new, corrected C_x (25°C) value.   The new IFC base values will generally have a greater than 2 or 3% effect on solar x-ray flux only in the lowest part of R0, near the channel thresholds.

11.2   Periodic Cross-Check of Different XRS Units

Two spacecraft are normally used as the operational GOES, so data from two XRS units are generally available.   The solar x-ray fluxes measured by these two XRS units are available to monitoring personnel, and any significant difference would be noticed. Periodic comparison of the two XRS unit fluxes would allow deviations to be detected at any early stage, before the differences could lead to operational uncertainties.

The two operational XRS units should generally be compared three or four times a year, with the data being used to determine any trends which could be used to predict the onset of deviations greater than 5 or 10%.   The comparisons should be made at near mid-range in R1 or R2, during a period of slowly varying solar x-ray fluxes.   Electron and proton fluxes should be low and R0 data should be avoided to reduce any possible particle contamina-

tion effects. The comparisons should be made with temperature-corrected calibration data. A long term plot of these comparisons can be used to determine when a deviation from agreement began, should a significant difference in flux develop.

A second, more detailed comparison should be made about once a year, during a Class X flare. This would allow detailed comparison of the operational XRS units over nearly all x-ray ranges, and at several points in each range. The data can be used to detect changes in each range, and to verify that range change discontinuities are stable (in-orbit calibration corrections should reduce such discontinuities to a few % of less - see Section 11.3).

A third comparison should also be attempted about once per year. Any additional standby GOES spacecraft should be operated as a third GOES and the XRS unit (if still operational) used for a third intercomparison. It would be preferable to make this comparison during a period of solar x-ray flare activity, if possible, but there should be at least a high R0 or R1 flux present to allow reliable intercomparison. This could be done over the course of a few weeks, using whichever GOES standby spacecraft are available. The results would give additional data on the long term XRS stability, particularly the ion chamber stability against gas leakage.

11.3   Normalization of Follow-On XRS Units

As shown in Section 9.2, two XRS units can give in-orbit measured solar x-ray fluxes that are as much as 20% different. To avoid operational uncertainties and to preserve the long term continuity of the GOES solar x-ray data, follow on XRS units have generally had the ground calibration constants normalized in-orbit to give agreement with the SMS-2 XRS data. This should be done routinely with a new XRS unit following the launch of a follow-on GOES.

The XRS calibration normalization requires at least a Class M and preferably a Class X flare. As shown in Section 9.2, the R1/R0 and R3/R2 range change discontinuities have generally been less than a few %, but the R2/R1 discontinuity has been as much as 20%. It is expected that most XRS units will require a single normalization factor for each channel (A and B), but it is possible that each channel may have separate factors R3 + R2 and R1 + R0. After detailed comparison to the <u>corrected</u> operational GOES XRS units, a set of correction factors as in Table 9.5 can be obtained for each new XRS following a GOES launch.

The XRS normalization process should not be used if the deviations are too large, since this could result in a long term shift, most likely a decrease because of ion chamber gas leakage. Since a new XRS can generally be compared with at least two older operational XRS units (and preferably a number of even older XRS units on standby GOES), a large positive deviation (new XRS fluxes significantly larger) is unlikely since it would require identical gas leak rates in all in-orbit XRS units. Should any

121

in-orbit XRS units develop a gas leak this is most likely to have been detected by the periodic comparisons recommended in Section 11.2.

Considering the past GOES XRS stability history, the most likely deviation of a new XRS is downward, with a gas leak in the new unit indicated. The could be verified by comparison of x-ray flux data over the next few months where the new XRS fluxes would show an increasingly greater deviation downward. Under such conditions the new XRS data would not be valid for the channel(s) showing the deviation.

Note that the channel A data from GOES-2, 4, 5 and 6 are all about 20% lower than SMS-2, so a $\pm$ 20% deviation allowance for follows-on XRS units should be relative to a 20% lower response for channel A (the channel A correction factor should be in the in the range of 1.2 ± 0.25). Any correction factor deviations of more than 20% (1.0 ± 0.2 for channel B) should be considered suspect until further investigation rules out gas leaks and other potential problems.

Ultimately, it may be necessary to renormalize the XRS fluxes to a new unit calibration. This would occur when two successive new XRS units both showed increased fluxes of more than 20% above the older units. At this point a more detailed investigation would be required to eliminate the possibility of ground calibration procedures being responsible for the increase, but if data showed that all older XRS units gave fluxes decreasing relative to the new units, then a new normalization would be required. However, it is felt that this is an unlikely occurrence because it requires identical leak rates, starting simultaneously, in at least two older XRS units. Normally, as gas leak in any one XRS unit would be detected by the periodic checks recommended in Section 11.2

12. CONCLUSIONS

The in-orbit operation of the particle detectors (EPS/HEPAD) and solar x-ray sensors (XRS) on the GOES-4, 5 and 6 spacecraft has been investigated in detail. The EPS/HEPAD data have been analyzed both for operational stability (the IFC data), and for particle response during solar proton events. Solar proton data have been compared with low altitude NOAA-8 data over the polar caps with reasonable flux agreement for the selected February 16, 1984 event.

The GOES-5 E1 channel electron flux data show a significant increase above the expected average fluxes during late 1984 and late 1985, so that after 5 years in orbit the integrated flux is about 50% greater than expected. This has led to radiation damage in the D3 dome detector, and indicates that the radiation dose at geosynchronous orbit may at times be significantly larger than expected from past average electron flux conditions.

The XRS data show good long term electronics stability from the IFC data, and x-ray flux comparisons between different XRS

122

units indicate a likely good stability in ion chamber response (< 5% gas leak over 5-6 years). XRS units require up to 20% renormalization of the ground calibration to minimize in-orbit disagreement in measured solar x-ray flux. This is near the estimated uncertainty in ion chamber calibration.

Several suggestions for normal in-orbit checks on EPS/HEPAD and XRS operation have been detailed. These involve primarily an expanded set of electronics checks with the EPS IFC data, and HEPAD gain adjustment for the PMT. The XRS checks include routine IFC checks, and periodic cross-checks are also made for normalization of the ground calibration constants for follow-on XRS units through comparison of in-orbit x-ray flux data.